J. Mech. Phys. Solids 176 (2023) 105308

Contents lists available at ScienceDirect

Journal of the Mechanics and Physics of Solids

journal homepage: www.elsevier.com/locate/jmps

A strain energy function for large deformations of compressible elastomers

Matteo Pelliciari [a], Stefano Sirotti [a,b,*], Angelo Marcello Tarantino [a]

[a] DIEF, Department of Engineering "Enzo Ferrari", via P. Vivarelli 10, 41125 Modena, Italy
[b] College of Civil Engineering, Fuzhou University, No. 2 Xue Yuan Road, 350108 Fuzhou, Fujian Province, PR China

ARTICLE INFO

Keywords:
Hyperelasticity
Rubber-like materials
Compressibility
Volumetric deformations
Experiments
Parameter fitting

ABSTRACT

Elastomers are typically considered incompressible or slightly compressible. However, we present simple tension and bulk tests showing that, under large deformations, these materials can undergo significant volume changes. A review of the literature reveals the lack of an accurate hyperelastic model for finite volumetric deformations of elastomers. Therefore, we propose a new volumetric strain energy density (SED) that overcomes the limitations of the current models. The main advantages of the proposed SED are: (1) accurate description of the response of rubbers for both small and large volumetric deformations; (2) ability to reproduce diverse behaviors during volume shrinkage and expansion; (3) adaptability to other compressible materials, such as soft tissues, foams and hydrogels. Using the deviatoric–volumetric split of the strain energy, the proposed volumetric SED is combined with a suitable deviatoric part selected from the literature. The parameters of the combined SED are calibrated by fitting the model to the experimental data from simple tension and bulk tests. As a result, an accurate description of the response of elastomers under both shape and volume deformations is provided. The proposed SED can be implemented in numerical codes to capture the effects of volumetric deformations on the equilibrium solutions for various stress states.

1. Introduction

Due to their ability to withstand large elastic deformations, elastomers have received a great deal of attention in engineering technology. Many applications can be found in the biomedical field, with a particular focus on tissue engineering for cardiac and vascular systems (Yang et al., 2004; Ye et al., 2018). The low weight and high stretchability of rubbers make them suitable for industrial applications such as insulation, tires, airbags and food packaging (Loew et al., 2019; Baschetti and Minelli, 2020). Seismic isolation devices are usually composed of elastomers, which are capable of absorbing much of the impact of an earthquake (Tsang, 2008). Rubber nanocomposites assumed great importance because of their many applications in day-to-day life and fields of engineering such as electronics and automotive (Liu et al., 2018; Sethulekshmi et al., 2022; Pelliciari and Tarantino, 2022). All the technological applications of elastomers involve large deformations and thus mechanical modeling requires concepts of finite elasticity.

The common approach in the modeling of elastomers is to consider these materials as incompressible. This is based on the observation that their bulk modulus is much larger than their shear modulus (Warfield et al., 1970; Boyce and Arruda, 2000; Mott et al., 2008). Such an assumption simplifies considerably the mathematical form of the equilibrium problems and therefore it has been adopted by many researchers (Khajehsaeid et al., 2013; Horgan, 2015; Zhang et al., 2022). However, even under the

* Corresponding author at: DIEF, Department of Engineering "Enzo Ferrari", via P. Vivarelli 10, 41125 Modena, Italy.
E-mail addresses: matteo.pelliciari@unimore.it (M. Pelliciari), stefano.sirotti@unimore.it (S. Sirotti), angelomarcello.tarantino@unimore.it (A.M. Tarantino).

https://doi.org/10.1016/j.jmps.2023.105308
Received 7 April 2023; Accepted 30 April 2023
Available online 8 May 2023

hypothesis of incompressibility, analytical solutions in finite elasticity have been derived only for simple stress states such as uniaxial and equibiaxial tension. Hence, material models for rubbers are generally implemented in finite element (FE) codes to solve more complex problems. The implementation of incompressible constitutive models results in serious convergence problems due to volumetric locking (Armero, 2000; Heisserer et al., 2008). In addition, several experimental tests indicated that some rubbers are actually compressible (Blatz and Ko, 1962; Starkova and Aniskevich, 2010; Kugler et al., 1990; Steck et al., 2019). Thus, some researchers developed compressible and slightly compressible models to overcome the above issues (Levinson and Burgess, 1971; Bischoff et al., 2001).

Horgan and Saccomandi (2004) developed a constitutive model for slightly compressible materials that reflects limiting chain extensibility. Peng et al. (2021) proposed an extension of the Mooney–Rivlin hyperelastic model introducing a term that takes into account compressibility. Lengyel et al. (2016) studied the interface crack between a compressible elastomer and a rigid substrate and found that the solution was sensitive to the bulk properties of the material. Li et al. (2008) adopted a compressible constitutive law for rubber-like materials to describe the evolution of damage due to the Mullins effect and the cavity growth process. Landis et al. (2022) analyzed the surface wrinkles and creases in constrained dielectric elastomers under electromechanical loading by assuming a compressible material model. Angeli et al. (2013) proposed analytical solutions for carbon fiber-reinforced isolators with compressible elastomer subjected to compression and bending.

The most convenient method to study compressible hyperelastic materials is to introduce the deviatoric–volumetric decoupling of the SED (Sansour, 2008). The advantage is that with this approach the isochoric and volumetric behaviors can be treated independently. Numerous studies in the literature have been focused on modeling the deviatoric material response (see, e.g., Ogden et al., 2004; Steinmann et al., 2012; Destrade et al., 2017; Mihai and Goriely, 2017; Singh and Racherla, 2022; Zhou et al., 2023), but only a few authors analyzed the volumetric behavior. In fact, only a few hyperelastic models for the volumetric contribution exist in the literature (Moerman et al., 2020). Likewise, numerous experimental tests have been carried out to derive the stress vs. stretch response of rubbers when subjected to large deformations. However, only a few experimental works focused on measuring the volumetric deformations (Adams and Gibson, 1930; Bridgman, 1945). As a consequence, there is still a lack of accurate descriptions of the volumetric response of elastomers under large strains, from both experimental and analytical points of view.

In the present work, we present simple tension and bulk (volumetric compression) tests carried out on four kinds of elastomers. During the simple tension tests, we measured both longitudinal and lateral stretches with digital image correlation (DIC). In this way, in addition to the stress vs. stretch curves, we detected also the volume changes during the deformation process. The combination of the results from simple tension and bulk tests gives the volumetric response of each rubber under both volume shrinkage and expansion. For small stretches, the rubbers analyzed are nearly incompressible. However, for large stretches, some of the specimens exhibit volume expansions up to 60% and volume shrinkage around 10%–15%. Therefore, the assumption of incompressibility may not be accurate when dealing with problems involving large deformations.

We review the current volumetric SED formulations available in the literature and we perform a fitting to the experimental data. We demonstrate that the current formulations are not capable of providing an accurate description of the volumetric response of rubbers under large deformations. Thus, we propose a new volumetric SED that overcomes the limitations of the current theories. The proposed model is fitted to the experimental data and the results show accurate predictions.

With the aim of coupling the volumetric and deviatoric contributions, we consider the most common incompressible strain energy functions from the literature and we select the most suitable one by comparing their performance. We couple the selected incompressible model with our proposed volumetric SED and we present the equilibrium solutions for compressible materials. A final fitting to the experimental data is performed, providing an accurate description of both deviatoric (shape changing) and volumetric responses. To the knowledge of the authors, the fitting of a SED that includes both deviatoric and volumetric contributions for large deformations and volume changes in rubbers has not been carried out yet.

2. Theoretical background and research methods

The mechanical response of rubbers is typically investigated in the context of finite elasticity, due to the capability of these materials to undergo large elastic deformations. Hyperelasticity and isotropy are the most common assumptions of the phenomenological models for rubber-like materials (Rivlin and Saunders, 1997; Haines and Wilson, 1979; Pelliciari et al., 2022). In hyperelasticity, the mechanical properties of the material are described by a SED function W. Under the assumption of isotropy, W is a symmetric function of the principal strain invariants or the principal stretches (Upadhyay et al., 2019), namely

$$W = W(I_1, I_2, I_3) = \tilde{W}(\lambda_1, \lambda_2, \lambda_3), \tag{1}$$

with I_1, I_2 and I_3 defined as

$$I_1 = \mathrm{tr}\mathbf{B} = \lambda_1^2 + \lambda_2^2 + \lambda_3^2, \quad I_2 = \frac{1}{2}\left[(\mathrm{tr}\mathbf{B})^2 - \mathrm{tr}\left(\mathbf{B}^2\right)\right] = \lambda_1^2\lambda_2^2 + \lambda_1^2\lambda_3^2 + \lambda_2^2\lambda_3^2, \quad I_3 = \det\mathbf{B} = \lambda_1^2\lambda_2^2\lambda_3^2, \tag{2}$$

where $\mathbf{B} = \mathbf{F}\mathbf{F}^T$ is the left Cauchy–Green deformation tensor, $\mathbf{F}$ is the deformation gradient, and λ_1, λ_2 and λ_3 are the principal stretches. In the following, we consider the principal strain invariants as independent variables.

The first Piola–Kirchhoff stress tensor is defined as

$$\mathbf{P} = \frac{\partial W}{\partial \mathbf{F}} = 2\left(\frac{\partial W}{\partial I_1} + I_1\frac{\partial W}{\partial I_2}\right)\mathbf{F} - 2\frac{\partial W}{\partial I_2}\mathbf{B}\mathbf{F} + 2I_3\frac{\partial W}{\partial I_3}\mathbf{F}^{-T}. \tag{3}$$

This tensor provides a measure of stress referred to the initial configuration. The true stress, which is referred to the deformed configuration, is provided by the Cauchy stress tensor

$$\mathbf{T} = \frac{1}{J}\mathbf{P}\mathbf{F}^T, \tag{4}$$

where $J = \sqrt{I_3} = \det \mathbf{F}$ measures the volume change during deformation.

Material incompressibility is an assumption usually accepted in the theory of rubber elasticity. In this case, the only admissible deformations are isochoric (Pucci and Saccomandi, 2002), namely $J = \lambda_1\lambda_2\lambda_3 = 1$. The SED is a function of I_1 and I_2 only, and the Cauchy stress tensor $\mathbf{T}$ is expressed by

$$\mathbf{T} = -p\mathbf{I} + 2\frac{\partial W}{\partial I_1}\mathbf{B} - 2\frac{\partial W}{\partial I_2}\mathbf{B}^{-1}, \tag{5}$$

where p is a pressure term introduced by the incompressibility constraint.

When dealing with compressible materials, volume changes are considered by defining the SED as a function of all three invariants I_1, I_2 and I_3 (or J). The general expression of the SED is

$$W = W_c\left(I_1, I_2, J\right) + W_h\left(J\right), \tag{6}$$

where W_c and W_h are respectively the compressible and the hydrostatic terms of the strain energy. Both terms contribute to the response to a volume change, whether or not J appears explicitly in W_c (Bischoff et al., 2001). The most convenient approach to develop phenomenological models for compressible materials is to introduce the so-called deviatoric strain invariants, defined as

$$\bar{I}_1 = J^{-2/3}I_1, \quad \bar{I}_2 = J^{-4/3}I_2. \tag{7}$$

This allows to write the SED as the sum of two uncoupled terms, responsible for the deviatoric (shape changing) and volumetric (volume changing) deformations. The SED assumes the form

$$W = W_d\left(\bar{I}_1, \bar{I}_2\right) + W_h\left(J\right), \tag{8}$$

where W_d is the deviatoric term of the strain energy. The deviatoric–volumetric split brings advantages in the material characterization because only W_h is responsible for the material response to pure volumetric deformations.

The Cauchy stress tensor reads

$$\mathbf{T} = \mathbf{T_d} + t_h\mathbf{I}, \tag{9}$$

being $\mathbf{T_d}$ the deviatoric part of the Cauchy stress, t_h the hydrostatic stress and $\mathbf{I}$ the identity tensor. The hydrostatic stress is defined as (Moerman et al., 2020)

$$t_h = \frac{1}{3}\mathrm{tr}(\mathbf{T}). \tag{10}$$

In case of the deviatoric–volumetric split, the hydrostatic stress can be directly computed as

$$t_h = \frac{dW_h(J)}{dJ}. \tag{11}$$

The above relations allow independent characterization of the volumetric part W_h on the basis of experimental tests in which the volume changes are measured. Combining Eqs. (10) and (11), the relation between the stress and W_h for the case of simple tension test becomes

$$\frac{1}{3}t_1 = t_h = \frac{dW_h(J)}{dJ}, \tag{12}$$

where t_1 is the principal Cauchy stress in the longitudinal direction, while the two lateral principal stresses are zero ($t_2 = t_3 = 0$). In the case of bulk (volumetric compression) testing of rubbers, as described in Appendix A.2, the expression of the principal stress in longitudinal direction becomes

$$t_1 \approx t_h = \frac{dW_h(J)}{dJ}. \tag{13}$$

2.1. Structure of this research

The steps and methods of the present research are summarized in the scheme of Fig. 1. A brief description of each step is provided in the following.

(1) Simple tension and bulk tests performed on four kinds of rubbers are presented. The stress vs. stretch curves and the t_h vs. J curves are obtained.
(2) The currently available volumetric SED formulations are analyzed and their limitations are discussed. Consequently, a new volumetric SED function that overcomes such limitations is proposed. The model parameters are fitted on the experimental t_h vs. J data.
(3) The most common strain energy functions for the deviatoric part of the SED are reviewed. Each model is fitted to the experimental data in simple tension and the most suitable formulation is selected.

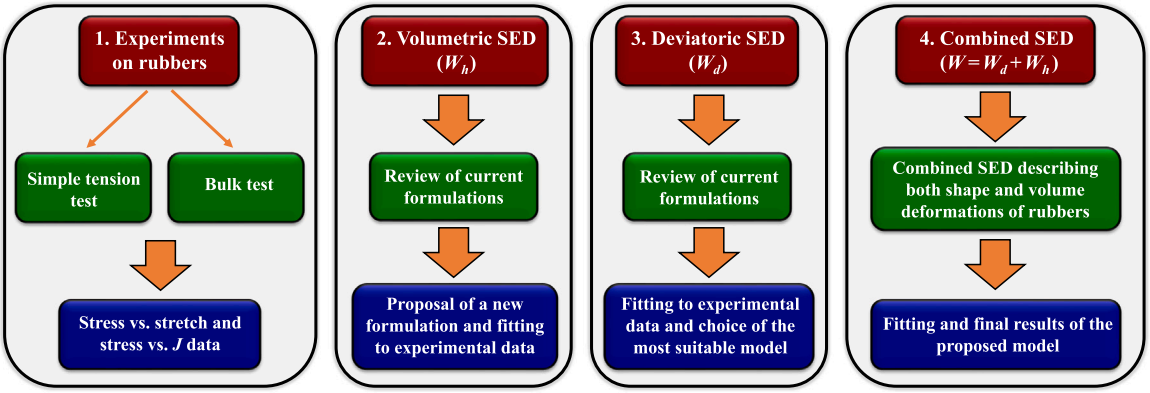

Fig. 1. Flowchart showing the steps and methods of the present work.

(4) The combined SED is obtained by assembling the deviatoric and the proposed volumetric parts. The model describes both shape and volume changes of compressible rubbers under large deformations.

The paper is organized as follows. In Section 3 we present the experimental tests, in which large volume changes in rubbers are observed. In Section 4 we review and analyze the most common volumetric SED formulations available in the literature. The results show that there is a need for an accurate model for large volume deformations of elastomers. Therefore, a novel volumetric SED formulation is proposed in Section 5. In Section 6 we select a suitable model for the deviatoric part of the SED by analyzing the ones available in the literature. The volumetric and deviatoric parts are combined and the final results are presented in Section 7. Finally, the conclusions are drawn in Section 8.

3. Experiments

In this section, we present simple tension tests and bulk tests carried out on four kinds of rubber: EPDM (ethylene propylene diene monomer), NBR (nitrile butadiene rubber), NR (natural rubber) and silicone.

3.1. Simple tension test

Three dogbone specimens were prepared for each rubber considered. The specimens had an effective length of 60 mm, a height of 7 mm and a thickness of 1 mm. The tests were performed using the testing machine Instron 5567. The elongation was applied with a displacement rate of 500 mm/min.

Digital image correlation was employed to monitor the displacement field during each test. In particular, as shown in Fig. 2(a), a Nikon D3200 camera was used to record a video throughout the experiment. The camera was positioned in front of the specimen with an orthogonal view, which was ensured by properly installing a tripod. The camera recorded a video of the test from the initial load application to the specimen failure. From the video, 100 frames were extracted with regular time intervals. The captured images were then imported to MATLAB and processed with the open-source DIC package *Ncorr* (Blaber et al., 2015).

A rectangular region of interest (ROI) was defined in the central part of the rubber specimen, where the strains are expected to be homogeneous. The dimension of the region of interest was 40 mm x 5.5 mm. The DIC analysis with *Ncorr* provided the displacement and strain fields in both longitudinal and lateral directions. Contour plots of the test on NBR are displayed in Fig. 3. We observe that inside the ROI both longitudinal and lateral strains ε_x and ε_y are homogeneous. Since *Ncorr* computes the Green–Lagrange strain components (Zheng et al., 2020), the corresponding values of stretch components were computed as $\lambda_x = \sqrt{1+2\varepsilon_x}$ and $\lambda_y = \sqrt{1+2\varepsilon_y}$. As a double check, the images were post-processed with the MATLAB application *Ncorr_post*. Virtual extensometers were placed inside the ROI along x and y directions. The software computed the relative displacements, from which stretches were calculated and it was checked that the strain fields were accurate.

The nominal stress σ_x was computed as F/A, where F is the force applied by the testing machine and A is the cross-section area of the specimen in the initial configuration (7 mm x 1 mm). In this way, the stress vs. stretch curve was derived from each test. For each rubber, three tests were carried out on the three specimens prepared. Since there was not much variation in the results of the three tests, we consider the average data of stretches and stresses.

The experimental data are displayed in Figs. 4(a) and 4(b) in terms of σ_x vs. λ_x and λ_y vs. λ_x curves, respectively. Fig. 4(b) shows a representation of the incompressible limit, expressed by $\lambda_y = 1/\sqrt{\lambda_x}$. We observe that the response of all four rubbers is very close to incompressibility for relatively small strains. EPDM and NBR start to deviate at values of longitudinal stretch around 1.35 and 1.15 respectively. On the other hand, NR and silicone are nearly incompressible throughout the deformation process and show sensible deviations only for very large deformations. The above behaviors are explained by the fact that both EPDM and NBR compounds contain a significant amount of specific fillers, such as carbon black. Instead, the amounts of filler in the NR and silicone

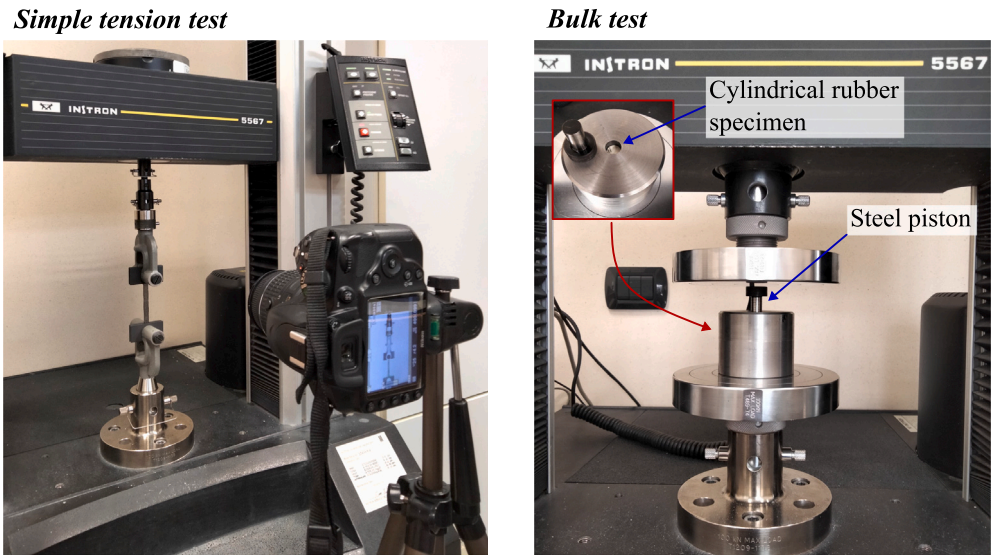

Fig. 2. Experimental tests on elastomers. (a) Simple tension test performed on a dogbone specimen. The test was monitored with a camera and the displacement field was obtained through digital image correlation (DIC). (b) Bulk test performed on a cylindrical specimen. The specimen was inserted into a rigid annulus and a steel piston was used to apply the axial load.

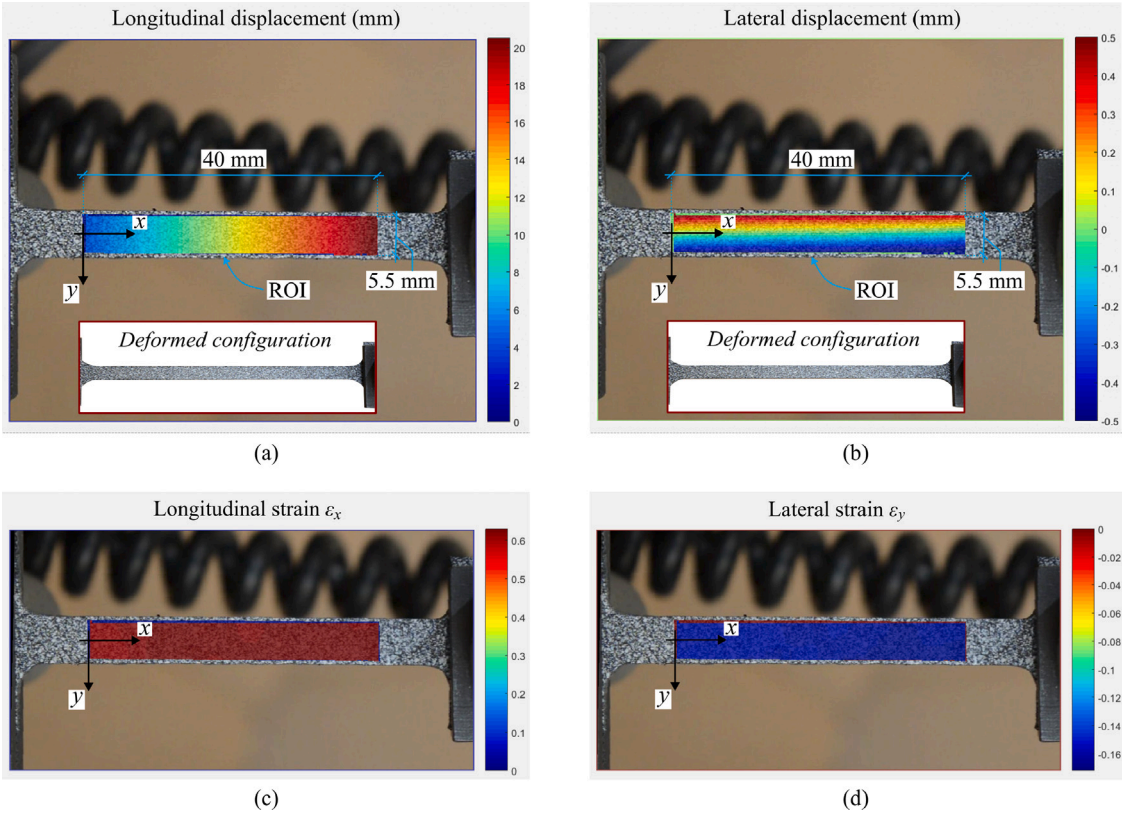

Fig. 3. Contour plots in the selected region of interest (ROI) obtained from DIC analysis with MATLAB software *Ncorr*. Figures (a) and (b) show respectively longitudinal and lateral displacement fields, while figures (c) and (d) show longitudinal and lateral strain fields, respectively. The plots are referred to the simple tension test on NBR at the step corresponding to longitudinal stretch $\lambda_x = 1.5$.

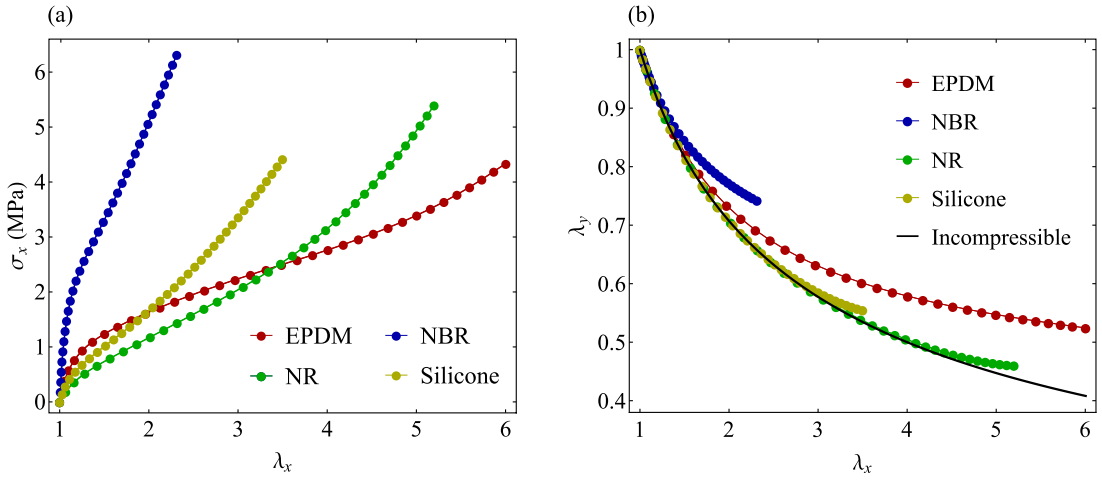

Fig. 4. Results from simple tension tests on EPDM, NBR, NR and silicone. (a) Nominal stress σ_x vs. longitudinal stretch λ_x and (b) lateral stretch λ_y vs. longitudinal stretch λ_x. The black curve shows the behavior of incompressible materials, expressed by $\lambda_y = 1/\sqrt{\lambda_x}$.

considered in this work are very low. A higher compressibility associated with an increase in filler content was observed also in other works (Gurvich and Fleischman, 2003; Omnès et al., 2008).

Only a few experimental measurements of the lateral deflection in rubbers were reported in the literature. The results of such experiments seem to agree with the ones presented in this work. Starkova and Aniskevich (2010) performed uniaxial tension tests on silica-filled SBR rubber and measured the Poisson's ratio ν during the experiments. They found out that for small stretches the response is close to incompressibility ($\nu \approx 0.5$), while for large deformations ν becomes stretch-dependent and the material is compressible. Kugler et al. (1990) considered five elastomers and reported measurements of volume changes during simple tension tests, which showed once again that compressibility increases with the deformation.

3.2. Bulk test

The bulk (or volumetric compression) test involves the application of an axial compressive load on a cylindrical specimen inserted into a rigid annulus. The deformation of the cylindrical specimen is homogeneous and the longitudinal stretch equals the volume change. In fact, the lateral deformation is constrained ($\lambda_y = \lambda_z = 1$) and we have that $\lambda_x = J$.

Three cylindrical specimens with a height of 12 mm and a diameter of 10.5 mm were prepared for each rubber. A cylindrical steel block with a circular hole was manufactured. The hole had a depth of 20 mm and a diameter of 10.55 mm. The rubber specimen was inserted into the hole so that its side walls were fixed. Note that the diameter of the hole in the steel block was slightly larger than that of the specimen so as to allow smooth insertion and removal.

As shown in Fig. 2(b), a steel piston with the same diameter as the cylindrical specimen was used to apply the axial load. The tests were performed by using the testing machine Instron 5567 equipped with a 30 kN load cell. A limit on the applied load was set to 26 kN, which corresponds to an axial stress on the specimen of around 300 MPa. The displacement was applied with a displacement rate of 2 mm/min. At the beginning of the test, the lateral walls of the specimen were still not perfectly constrained by the rigid annulus, due to a slightly smaller diameter. Thus, the data until an applied force of 4 N were removed. Such a force corresponds to an axial stress of approximately 0.05 MPa. This cut-off value was defined by computing the axial stress corresponding to a lateral strain of 0.48%, which is the condition where the specimen touches the internal walls of the rigid annulus. Since the strains are still small, this simple computation was done by assuming a linear elastic response with Poisson's ratio 0.5 and Young's modulus 5 MPa.

The force vs. displacement data were converted into stress vs. stretch data. In this test, the nominal stress σ_x is equal to the true stress t_x. Hence, for convenience in the following analysis, the results are given in Fig. 5(a) in terms of true stress as a function of J. The curves show that, at the maximum level of stress, all four rubbers undergo large volumetric changes (up to 10%–15% of shrinkage).

The above results show the response of the rubbers in terms of t_x vs. J curve when $J < 1$ (shrinkage). To have a comprehensive picture of the volumetric changes in the materials, we extracted the t_x vs. J curve from the experimental data from the simple tension tests, which show the response when the volume is expanding ($J > 1$). The results are shown in Fig. 5(b).

As discussed in detail in Appendix A.2, it can be assumed that for rubber-like materials the axial stress measured during the bulk test is approximately equal to the hydrostatic stress ($t_h \approx t_x$). In light of this, the bulk modulus κ was derived from the slope of the experimental data from bulk tests in the small-strain domain. In shrinkage, the range of small strains was identified by observing until what magnitude of deformation the material response was still approximately linear. For the rubbers considered, the linear behavior is restricted to a shrinkage of 2‰. The estimated values of κ are reported in Table 1 and a detail of the experimental data from bulk tests in the small-strain region is shown in Fig. 6.

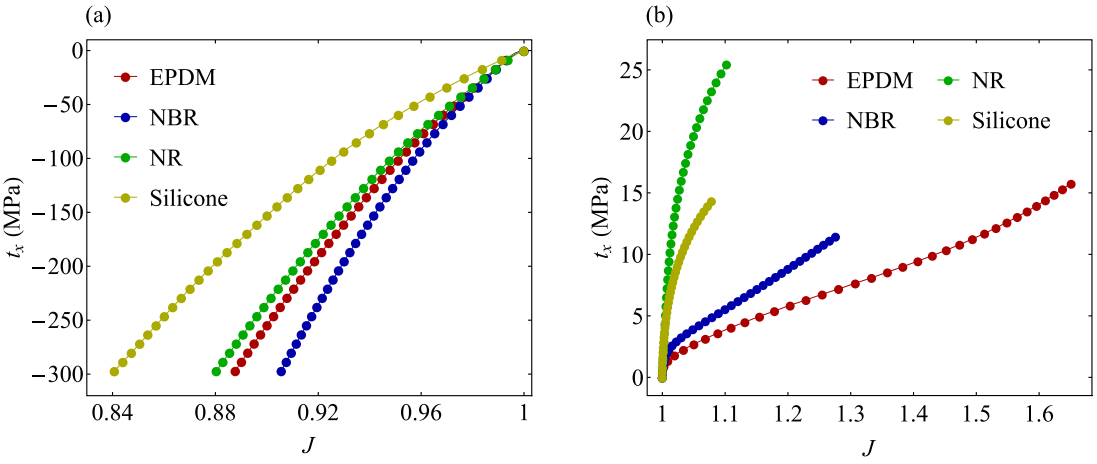

Fig. 5. Cauchy stress t_x as a function of volume change J from experimental tests on EPDM, NBR, NR and silicone. Figure (a) shows the response obtained from the bulk tests, where the specimens are subjected to shrinkage ($J < 1$), while figure (b) shows the response from simple tension tests, where the volume of the specimens is expanding ($J > 1$).

Table 1
Values of bulk modulus κ calibrated from the experimental data from bulk tests in the small-strain domain (up to a shrinkage of 2‰).

Rubber	EPDM	NBR	NR	Silicone
κ (MPa)	490	410	710	670

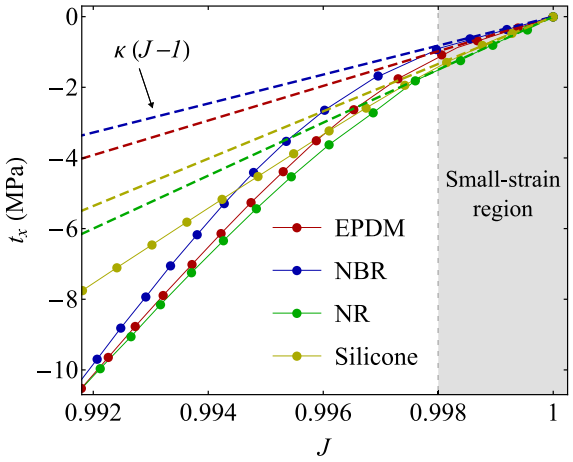

Fig. 6. Detail of the experimental data from bulk tests. The values of bulk modulus reported in Table 1 were calibrated in the small-strain region, up to a shrinkage of 2‰, where the response of all the rubbers is approximately linear. The dashed lines represent the linear response given by $\kappa(J-1)$.

4. Current formulations for the volumetric part of the SED

Taking advantage of the decomposition of the strain energy function, expressed in Eq. (8), several researchers proposed formulations for the volumetric part W_h of the SED to capture the volumetric response of solids under large volumetric changes. Firstly, we give a brief description of the most significant formulations found in the literature. Then, we analyze the capability of such formulations to model the volumetric response of rubbers. To do this, we fit each model to the experimental data presented in the previous section.

We recall that for the bulk test on rubber-like materials, we can assume that $t_h \approx t_x$. As regards the experimental t_x vs. J curves from simple tension tests reported in Fig. 5(b), the hydrostatic stress is derived as $t_h = t_x/3$ (see Eq. (12)). Hence, the experimental data from both bulk and simple tension tests shown in Fig. 5 are converted in t_h vs. J curves. We will refer to these experimental curves throughout this section.

Table 2
Current volumetric SED formulations from the literature.

Formulation	$W_h(J)$
Hencky (1933)	$\frac{\kappa}{2}\ln(J)^2$
Simo (1988)	$\frac{\kappa}{2}(J-1)^2$
Doll and Schweizerhof (2000)	$\frac{\kappa}{\alpha+\beta}\left(\frac{1}{\alpha+1}J^{\alpha+1}+\frac{1}{\beta-1}J^{-(\beta-1)}\right)-\frac{\kappa}{(\alpha+1)(\beta-1)}$
Montella et al. (2016)	$\frac{\kappa}{2\beta_1}\left(e^{\beta_1\ln(J)^2}-1\right)+\frac{\kappa_2}{m\beta_2}\left(e^{\beta_2\lvert\ln(J)\rvert^m}-1\right)$
Moerman et al. (2020), No. 3	$\kappa\left[-(1-q)a^2\ln\left(\cos\left(\frac{J-1}{a}\right)\right)+qb^2\ln\left(\cosh\left(\frac{J-1}{b}\right)\right)\right]$

4.1. Review of current formulations

Table 2 gathers the most common volumetric SED formulations, which are discussed in the following. The two functions proposed by Hencky (1933) and Simo (1988) are implemented in many finite element codes. Their success lies in their mathematical simplicity. However, despite providing good performance for nearly-incompressible materials ($J \approx 1$), they lead to unrealistic behaviors when dealing with large volumetric changes.

Doll and Schweizerhof (2000) proposed a three-parameters volumetric function that allows control in both shrinkage and expansion through parameters α and β. In their work, the authors established 9 criteria that should be fulfilled by the volumetric SED to ensure physically consistent behavior of the material during shrinkage and expansion (see Table 2 in Doll and Schweizerhof (2000)). To satisfy such criteria, the constraints on parameters α and β are: $\alpha > 0$ and $\beta > 1$. Parameter α increases the response in expansion while slightly limiting the response in shrinkage, whereas parameter β produces the opposite effect. Note that the control on the response in shrinkage and expansion is not independent, since α and β have an effect on both branches.

Montella et al. (2016) proposed a five-parameters formulation developed starting from the exponentiated Hencky strain energy, firstly presented by Neff et al. (2015). The 9 criteria established in Doll and Schweizerhof (2000) are respected with the following constraints on the model parameters: $\beta_1 \geq 1/8$, $\beta_2 \geq 1/8$, and $m > 2$. This formulation does not offer independent control on the response for shrinkage and expansion.

Moerman et al. (2020) added a tenth requirement to the 9 described by Doll and Schweizerhof, which states that the volumetric part of a hyperelastic model should be capable of describing strain stiffening for all values of J. This means that the control of strain stiffening should be independent for shrinkage and expansion. In Moerman et al. (2020), the authors proposed three novel formulations for the volumetric strain energy function. Formulation No. 3, which is the most refined one, involves three parameters a, b and q that assume different values for expansion and shrinkage. In particular, the parameters are defined as

$$a = \frac{2}{\pi}\begin{cases} J_1 - 1, & J \geq 1 \\ J_2 - 1, & J < 1 \end{cases} \qquad b = \frac{1}{\kappa}\begin{cases} s_1, & J \geq 1 \\ s_2, & J < 1 \end{cases} \qquad q = \begin{cases} q_1, & J \geq 1 \\ q_2, & J < 1 \end{cases} \tag{14}$$

This ensures that the formulation offers a completely independent control of the two branches. Including κ, the parameter values that must be calibrated are 7. More details about all the above formulations can be found in Moerman et al. (2020).

In the following, we fit the volumetric SED formulations to the experimental data presented in Section 3 for EPDM, NBR, NR and silicone. The simple formulations proposed by Hencky (1933) and Simo (1988) do not fulfill the previously mentioned criteria of physical plausibility. Hence, we will not report the results obtained with such formulations. In addition, it is obvious that the other formulations that involve more parameters will provide a better response.

It goes without saying that in the literature there are other volumetric SED models in addition to those considered in this work. For instance, the formulations proposed by Bischoff et al. (2001), Ogden (1972), Hill (1979), and Horgan and Murphy (2009b). However, such formulations do not fulfill all the criteria of physical plausibility and provide accurate behaviors only for small or moderate volume changes. Hence, they are not capable of accurately reproducing the response of the rubbers analyzed in this work during both volume shrinkage and expansion. For the above reasons, they were not considered in this work.

4.2. Fitting to experimental data

The hydrostatic stress was computed as $t_h = dW_h/dJ$ for each of the volumetric SED formulations described above. The analytical expression was fitted to the experimental data from simple tension and bulk tests by using the *FindFit* function in software *Wolfram Mathematica*.

For each rubber, the bulk modulus was fixed to its corresponding value given in Table 1. To perform an in-depth study of the advantages and limitations of each material model for both shrinkage and expansion, the fitting was done by considering separately the experimental data for $J < 1$ and $J >$. Hence, two sets of calibrated parameters were obtained for each formulation (note that the formulation by Moerman et al. already involves two values for each parameter). The calibrated parameters are reported in Table B.4 and the t_h vs. J curves for each type of rubber are displayed in Fig. 7.

From Figs. 7(a), 7(c), 7(e) and 7(g), we observe that none of the current formulations provides accurate results when the volume of the rubber specimens is shrinking. This happens because most of the formulations were defined to capture the volumetric response

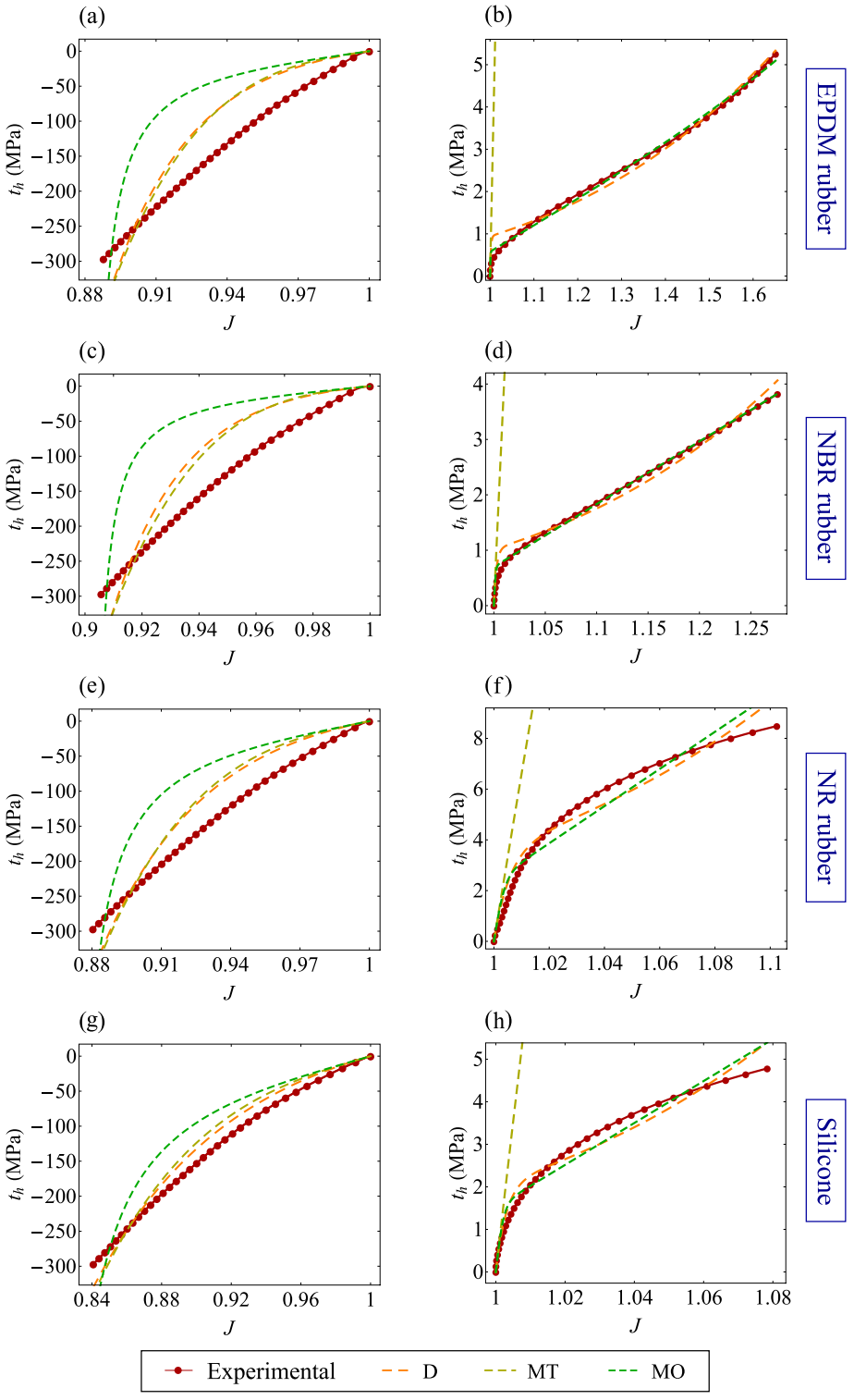

Fig. 7. Fitting of current volumetric SED formulations to the experimental data from bulk tests (Figs. (a), (c), (e) and (g)) and simple tension tests (Figs. (b), (d), (f) and (h)) for (a) and (b) EPDM, (c) and (d) NBR, (e) and (f) NR, and (g) and (h) silicone. The following acronyms are used: D = Doll and Schweizerhof (2000); MT = Montella et al. (2016); MO = Moerman et al. (2020).

of foams and hydrogels, which is substantially different from the response of elastomers. The elastic volume reductions in foams and hydrogels can reach easily values around 60 – 80% (Bardy et al., 2005; Petre et al., 2006) and strain stiffening typically takes place in a smooth way. On the other hand, starting from the initial configuration at $J = 1$, elastomers show a pronounced strain stiffening for small reductions of J. Then, the rate of stiffening decreases and stabilizes.

Figs. 7(b) and 7(d) show the behavior of EPDM and NBR when the volume is expanding. Except for the formulation by Montella et al., the current formulations give quite accurate descriptions of the volumetric response. However, as shown in Figs. 7(f) and 7(h), for NR and silicone the predictions are inaccurate. This happens because the rubbers are nearly incompressible when $J \approx 1$, then they show an abrupt reduction in stiffness (softening) that takes place for relatively low values of J. The description of such behavior requires a high degree of nonlinearity. For instance, the SED proposed by Moerman et al. is perfectly capable of reproducing both strain softening and stiffening in foams, which occurs smoothly and generally for much larger volume changes. However, the response of elastomers requires functions that capture these behaviors for smaller deformations and thus more rapidly.

In light of the above considerations, there is still a lack of a formulation that gives a comprehensive description of the volumetric response of elastomers. In the next section, we propose a new function that overcomes the limitations of the formulations currently available in the literature.

5. The proposed volumetric SED

The main limitations of the formulations currently available in the literature are the following:

- Most of them were developed for foams and hydrogels, therefore they do not accurately reproduce the volumetric response of elastomers. The main reason for this is that elastomers show pronounced strain stiffening and softening even for relatively small volume variations ($J \approx 1$).
- The formulations do not allow independent control of strain stiffening in shrinkage and expansion, except from the one proposed by Moerman et al. (2020).
- The above formulation involves parameters that assume two different values for $J < 1$ and $J \geq 1$, but the form of the energy function is the same. For rubbers, and perhaps other materials, it is convenient to have two different response functions defining the diverse behaviors in shrinkage and expansion.

In this section, we propose a new volumetric SED function that overcomes the limitations described above. The aim is to develop a formulation that gives an accurate description for both small and large volume changes.

5.1. The proposed function

The proposed volumetric SED is expressed by

$$W_h(J) = \kappa \left[H(1-J)\Psi_c + H(J-1)\Psi_t \right], \tag{15}$$

where H is the Heaviside step function, defined as

$$H(x) = \begin{cases} 0, & x < 0 \\ 1/2, & x = 0 \\ 1, & x > 0 \end{cases} \tag{16}$$

and Ψ_c and Ψ_t, which control shrinkage and expansion respectively, are expressed by

$$\Psi_c(J) = \frac{1}{\alpha_1 + \alpha_2 - \alpha_3} \left[\left(J + \frac{J^{\alpha_1+1}}{\alpha_1+1} + \frac{J^{-(\alpha_2-1)}}{\alpha_2-1} - \frac{J^{\alpha_3+1}}{\alpha_3+1} \right) - \left(1 + \frac{1}{\alpha_1+1} + \frac{1}{\alpha_2-1} - \frac{1}{\alpha_3+1} \right) \right], \tag{17}$$

$$\Psi_t(J) = (1-q) \left[\frac{\beta_2 e^{\beta_1(J-1)} + \beta_1 e^{-\beta_2(J-1)}}{\beta_1\beta_2(\beta_1+\beta_2)} - \frac{1}{\beta_1\beta_2} \right] + q\beta_3^2 \ln\left(\cosh\left(\frac{J-1}{\beta_3} \right) \right). \tag{18}$$

The use of the Heaviside step function allows an independent control of shrinkage and expansion. When $J < 1$, $H(J-1)$ vanishes and $H(1-J)$ equals 1, therefore the energy reduces to $\kappa\Psi_c$. On the contrary, when $J > 1$, $H(1-J)$ vanishes and $H(J-1) = 1$. Hence, the energy reduces to $\kappa\Psi_t$.

The hydrostatic stress for this formulation is[1]

$$t_h(J) = \frac{dW_h(J)}{dJ} = \kappa \left[H(1-J)\psi_c + H(J-1)\psi_t \right] \tag{19}$$

with

$$\psi_c(J) = \frac{d\Psi_c(J)}{dJ} = \frac{1 + J^{\alpha_1} - J^{-\alpha_2} - J^{\alpha_3}}{\alpha_1 + \alpha_2 - \alpha_3}, \tag{20}$$

[1] From the derivative of the product, the two terms $\delta(1-J)\Psi_c$ and $\delta(J-1)\Psi_t$ arise, where δ is the Dirac delta function. The above terms vanish because $\Psi_c\big|_{J=1} = \Psi_t\big|_{J=1} = 0$ and therefore the distributional products are identically zero.

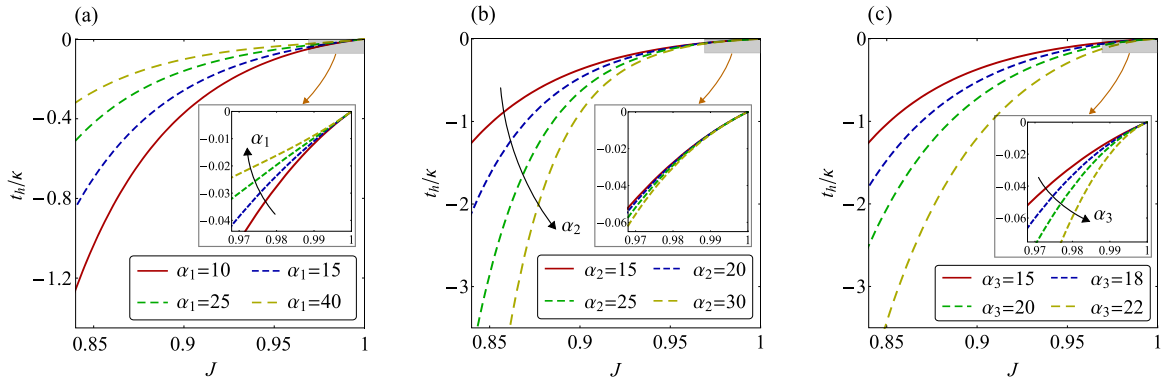

Fig. 8. Effect of parameters α_1, α_2 and α_3 of the proposed volumetric SED, which control the behavior for volume shrinkage. Parameters α_1 (a) and α_3 (c) are responsible respectively for strain softening and stiffening in the region of small to moderate shrinkage. Parameter α_2 (b) controls hardening during large volume shrinkage, while it has very little effect for small and moderate deformations. The curves are drawn starting from $\alpha_1 = 10$, $\alpha_2 = 15$ and $\alpha_3 = 15$, then the parameters are varied one by one.

$$\psi_t(J) = \frac{d\Psi_t(J)}{dJ} = (1-q)\frac{e^{\beta_1(J-1)} - e^{-\beta_2(J-1)}}{\beta_1+\beta_2} + q\beta_3 \tanh\left(\frac{J-1}{\beta_3}\right). \tag{21}$$

The expression of the hydrostatic stress shows yet again that the Heaviside step function guarantees a separate control on shrinkage and expansion, regulated by ψ_c and ψ_t respectively. Due to its discontinuity in $J = 1$, in practical implementations the Heaviside step function is sometimes replaced by a smooth approximation (Liang et al., 2020). In Appendix C we propose a sigmoid function to be used for this purpose.

Overall, the model involves seven parameters in addition to the bulk modulus. Parameters α_1, α_2 and α_3 control the response in shrinkage, while β_1, β_2, β_3 and q control the response in expansion. As discussed in detail in Appendix D, the proposed SED fulfills the 10 requirements reported in Moerman et al. (2020). The parameters have the following constraints:

$$\begin{cases} \beta_1 > 0,\ \beta_2 > 0,\ \beta_3 > 0,\ 0 \le q < 1 \\ \alpha_1 > 0,\ \alpha_2 > 1,\ \alpha_3 > 0,\ \alpha_1 + \alpha_2 - \alpha_3 > 0 \end{cases} \tag{22}$$

The term ψ_c in the hydrostatic stress, given in Eq. (20), comes from an improvement of the formulation proposed by Doll and Schweizerhof (2000), at which parameter α_3 was added. The effect of parameters α_1, α_2 and α_3 is displayed in Fig. 8. Parameters α_1 and α_3 produce, respectively, strain softening and stiffening in the range of small to moderate volume shrinkage. Parameter α_2 controls hardening for large volume changes. The combination of parameters α_1 and α_3 allows us to model the rapid strain stiffening that occurs in rubbers for relatively small shrinkage values.

The term ψ_t in the hydrostatic stress, given in Eq. (21), is inspired by the formulation proposed by Moerman et al. (2020). In such a formulation, the authors used functions *tan* and *tanh* to create vertical and horizontal sigmoid functions that simulate hardening and softening, respectively. However, the *tan* function is not suitable for the nonlinear behavior of elastomers, and thus it was replaced by the sum of two exponential functions with exponents β_1 and β_2. The effect of parameters β_1, β_2, β_3 and q is displayed in Fig. 9. Parameter β_1 produces strain stiffening at large volume expansions. The range of J values at which strain stiffening activates is regulated by parameter β_2. Parameter β_3 controls the amplitude of the linear response in small deformations. Finally, q is a weight parameter that regulates the transition from linear to nonlinear responses.

We remark that the proposed volumetric SED involves just one more parameter than the function proposed by Moerman et al. (2020). Its main advantages are the following:

- The proposed SED is a continuous function of J that was developed specifically for elastomers by observing their experimental behavior under large volume deformations.
- The Heaviside step function (or its smooth approximation) allows independent control of shrinkage and expansion.
- The formulation allows defining not only different parameters for shrinkage and expansion, but also different response functions. Since elastomers show different volumetric responses for $J < 1$ and $J > 1$, the two functions ψ_c and ψ_t were employed.
- When dealing with volumetric deformations of other hyperelastic materials, the response functions ψ_c and ψ_t can be replaced by other expressions if necessary.

5.2. Fitting the proposed SED formulation to the experimental data

The expression of the hydrostatic stress t_h as a function of J, reported in Eq. (19), was fitted to the experimental data by using the *FindFit* function in software *Wolfram Mathematica*. For each rubber, the value of bulk modulus is given in Table 1. The calibrated parameters are listed in Table B.5 and the t_h vs. J curves for each type of rubber are displayed in Fig. 10.

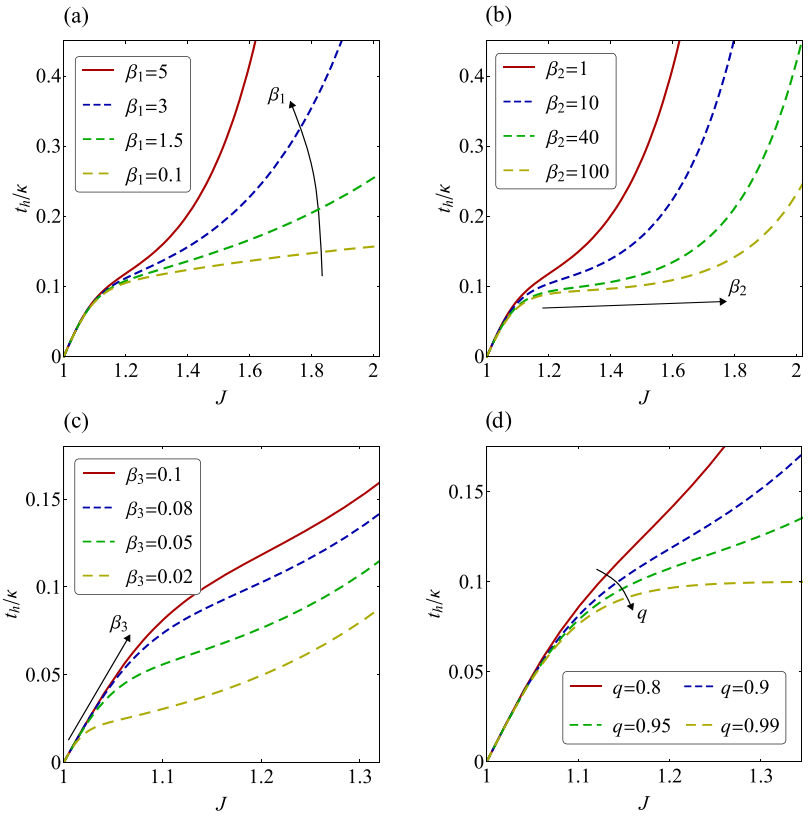

Fig. 9. Effect of parameters β_1, β_2, β_3 and q of the proposed volumetric SED, which control the behavior for volume expansion. Parameter β_1 (a) regulates the amount of hardening at large volume expansions, while β_2 (b) controls the activation of the hardening in the range of moderate deformations. Parameter β_3 (c) controls the extent of the linear response and q (d) governs the transition from linear to nonlinear responses. The curves are drawn starting from $\beta_1 = 5$, $\beta_2 = 1$, $\beta_3 = 0.1$ and $q = 0.9$, then the parameters are varied one by one.

We observe that, for all the rubbers, the proposed formulation provides accurate descriptions of both responses for volume shrinkage and expansion. In the case of shrinkage, elastomers show a rapid strain stiffening that occurs for small volume changes. This effect is captured thanks to the introduction of the new parameter α_3 in function ψ_c. In the case of volume expansion, elastomers are nearly incompressible when $J \approx 1$ and then an abrupt softening takes place, which is in some cases followed by hardening for large values of J. The exponential terms introduced in function ψ_t, controlled by parameters β_1 and β_2, allow reproducing such a behavior. Unlike the formulations currently available in the literature, the proposed model is capable of describing the volumetric response of rubbers for both small and large deformations.

6. The deviatoric part of the SED

Extensive studies were carried out on strain energy functions for the deviatoric (shape-changing) material response of rubbers. The goal of this section is not to propose a new formulation, but rather to find the most suitable one for the prediction of the response of elastomers under large deformations. To this purpose, firstly we review the most common incompressible strain energy formulations from the literature, then we fit each model to the experimental results in simple tension.

In the developments of this section, we adopt the assumption of incompressibility to investigate which material model provides the best prediction of the uniaxial response of rubbers, which involves shape-changing deformations. After having determined which deviatoric SED formulation is the most suitable, we combine it with the proposed volumetric SED presented in the previous section. The discussion on the final combined formulation will be presented in the next section.

6.1. Review of current incompressible strain energy functions for elastomers

The invariant-based hyperelastic material models are developed as functions of the first invariant or both the first and second invariants. The generalized Rivlin model (Rivlin and Saunders, 1997) is the foundation of many of the hyperelastic material laws. It is expressed by

$$W_d\left(I_1, I_2\right) = \sum_{i=0}^{n}\sum_{j=0}^{m} C_{ij}\left(I_1-3\right)^i\left(I_2-3\right)^j. \tag{23}$$

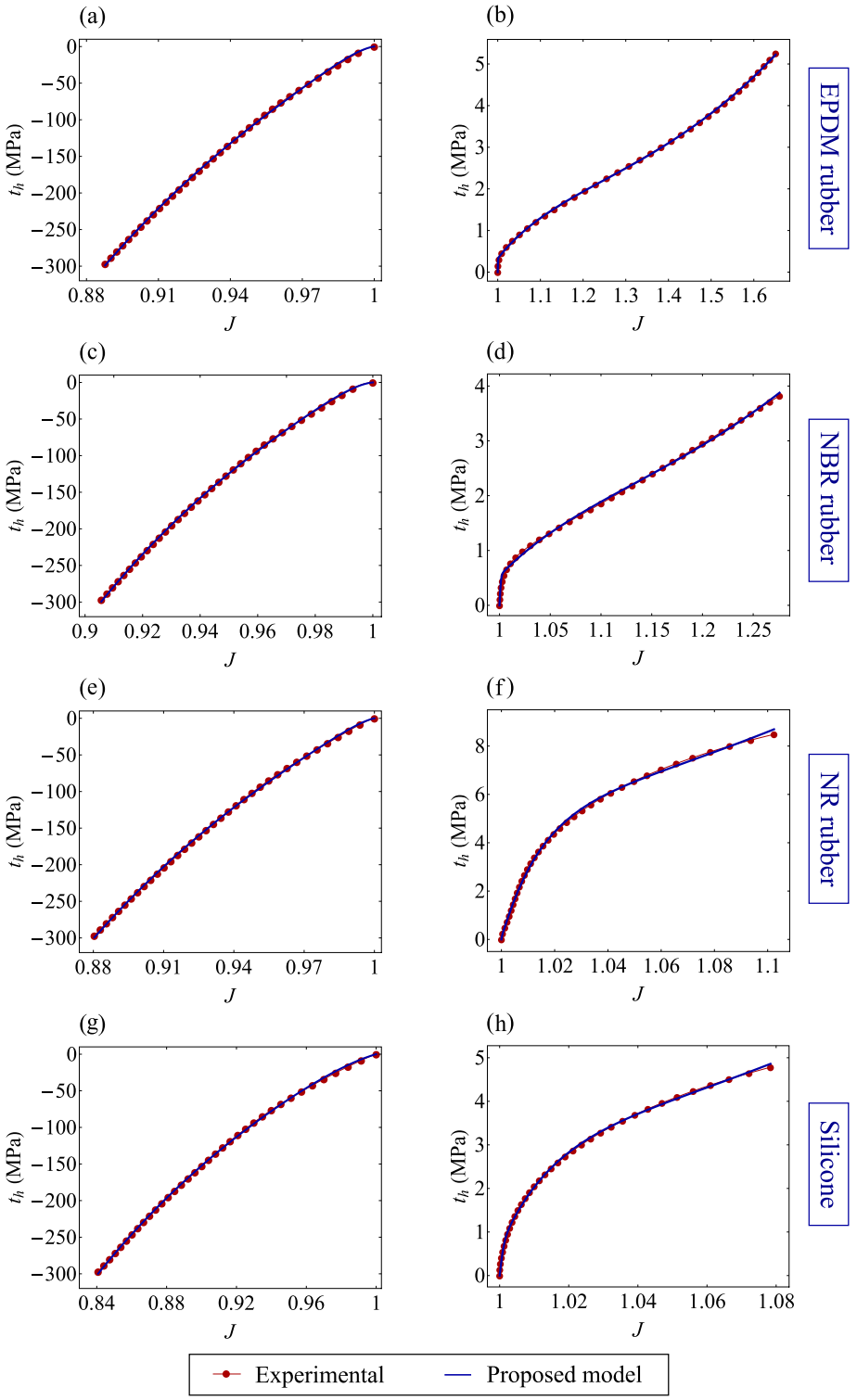

Fig. 10. Fitting of the proposed volumetric SED formulation to the experimental data from bulk tests (Figs. (a), (c), (e) and (g)) and simple tension tests (Figs. (b), (d), (f) and (h)) for (a) and (b) EPDM, (c) and (d) NBR, (e) and (f) NR, and (g) and (h) silicone.

In the following, we present a brief review of common hyperelastic models. Their analytical expressions are summarized in Table 3. Since our only goal here is to select a hyperelastic model that is reasonably accurate for rubbers in simple tension, we limit our study to models that involve at most 4 parameters.

Table 3
Common deviatoric SED formulations from the literature.

Formulation	W_d
Neo-Hookean (Treloar, 1943)	$C_{10}\left(I_1-3\right)$
Mooney–Rivlin (Rivlin, 1948)	$C_{10}\left(I_1-3\right)+C_{01}\left(I_2-3\right)$
Yeoh (Yeoh, 1990)	$C_{10}\left(I_1-3\right)+C_{20}\left(I_1-3\right)^2+C_{30}\left(I_1-3\right)^3$
Gent (Gent, 1996)	$-\frac{\mu}{2}J_m\ln\left(1-\frac{I_1-3}{J_m}\right)$
Gent-Gent (Pucci and Saccomandi, 2002)	$-C_1J_m\ln\left(1-\frac{I_1-3}{J_m}\right)+C_2\ln\left(\frac{I_2}{3}\right)$
Yeoh–Fleming (Yeoh and Fleming, 1997)	$\frac{A}{B}\left(I_m-3\right)\left(1-e^{-B(I_1-3)/(I_m-3)}\right)-C_{10}\left(I_m-3\right)\ln\left(1-\frac{I_1-3}{I_m-3}\right)$
Carroll (Carroll, 2011)	$AI_1+BI_1^4+CI_2^{1/2}$
Ogden (Ogden, 1972)	$\sum_{i=1}^{M}\frac{\mu_i}{\alpha_i}\left(\lambda_1^{\alpha_i}+\lambda_2^{\alpha_i}+\lambda_3^{\alpha_i}-3\right)$

The simplest among the invariant-based models is the neo-Hookean model (Treloar, 1943), defined as a linear function of the first invariant I_1. This function is based on considerations of the statistical molecular theory. Another classical SED for incompressible materials is the Mooney–Rivlin model (Rivlin, 1948). In addition to the dependence on the first invariant, it involves a linear dependence on the second invariant I_2, producing a deviation from the predictions of the molecular theory. The neo-Hookean and Mooney–Rivlin models have been widely employed for their simplicity. However, it is well-known that they do not provide accurate descriptions of the response of rubbers at large strains (Sirotti et al., 2023). In particular, these models are not able to simulate the hardening in the stress vs. stretch curve, which is a typical phenomenon observed in most rubber-like materials for technological applications. Hence, by analyzing the response of carbon-black-filled rubbers in simple tension, Yeoh (1990) proposed a three-parameter model defined by a combination of the first three powers of invariant I_1. This model is capable of describing the increase of stiffness at large deformations.

One of the most successful phenomenological models to reproduce severe strain stiffening is the one proposed by Gent (1996). The Gent model corrects the neo-Hookean model by introducing a maximum achievable length of the molecular chains. Parameter J_m denotes the chain extensibility limit. This model has the advantage of mathematical simplicity because it involves just two constitutive parameters. However, several authors pointed out that it is not capable of providing an accurate prediction of the response for the full range of deformations (Horgan, 2015). In particular, the Gent model is not accurate for small and moderate strains.

In view of this, modifications of the Gent model involving more constitutive parameters were proposed in the past. The most famous one is the so-called Gent-Gent model (Pucci and Saccomandi, 2002), which introduces a logarithmic dependence on the second strain invariant. Another modification was proposed by Yeoh and Fleming (1997). The authors combined concepts proposed by Yeoh and Gent in order to derive a comprehensive SED that is accurate for both small and large strains. The model proposed in Yeoh and Fleming (1997) depends only on the first strain invariant but it involves four parameters. A more recent model composed of three parameters was proposed by Carroll (2011). The model was derived by considering firstly the neo-Hookean function and then adding terms to model the residual stress in experimental data from simple and equibiaxial extensions.

Lastly, we must mention the well-known hyperelastic model proposed by Ogden (1972). It consists of a combination of terms depending on the principal stretches raised to variable powers. For consistency with the linearized theory, the constants must satisfy the following requirement: $\sum_{i=1}^{M}\mu_i\alpha_i=2\mu$, where M is a positive integer and μ is the shear modulus.

6.2. Fitting of the incompressible models to the experimental data

Among the incompressible SED formulations listed in Table 3, we limited our attention to the Gent model, the Gent-Gent model, the Yeoh model, the Carroll model, the Yeoh–Fleming model, and the Ogden model with $M=2$. The neo-Hookean and Mooney–Rivlin models were not considered because, as previously mentioned, they are not adequate to describe the response for large stretches. We fitted the above incompressible SED formulations to the experimental stress vs. strain curves derived from the simple tension tests (Fig. 4(a)). The analytical stress–strain relation for incompressible materials in simple tension is reported in Appendix A.1. The fitting was carried out by means of the *FindFit* function in *Wolfram Mathematica*. Note that for the Ogden model, we chose $M=2$ because we are considering formulations with at most 4 parameters.

The fitting parameters for each formulation are reported in Table B.6. Fig. 11 shows the results of the fitting for the four rubbers analyzed in this work. From Fig. 11(a) we observe that, except for the Gent and Yeoh models, all the formulations provide accurate descriptions of the response of EPDM rubber. However, Fig. 11(b) shows that only the Yeoh–Fleming model is capable of reproducing the behavior of NBR. All the other models are inaccurate, especially in the range of small to moderate strains (λ_x between 1 and 1.3). The results in the case of silicone shown in Fig. 11(d) confirm the above observation. Note that the Yeoh–Fleming model has four parameters, whereas the Gent-Gent, Carroll, and Yeoh formulations only have three. Thus, the better performance of the Yeoh–Fleming model is not surprising. However, the Ogden model counts for four parameters as well but it still shows severe limitations. We recall that the Yeoh–Fleming model was devised by combining two terms: one responsible for small strains and the

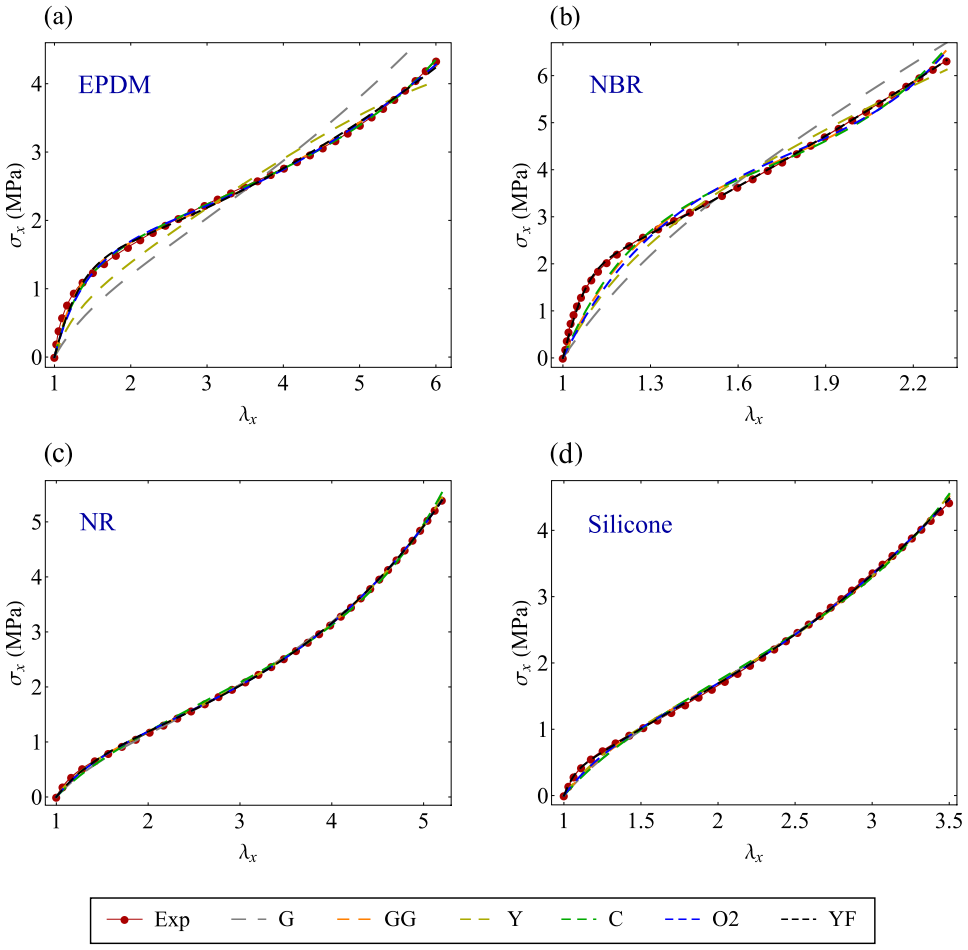

Fig. 11. Nominal stress vs. stretch curves obtained by fitting the current incompressible deviatoric SED formulations to the experimental data from simple tension tests on (a) EPDM, (b) NBR, (c) NR and (d) silicone. The following acronyms are used: Exp = experimental; G = Gent (Gent, 1996); GG = Gent-Gent (Pucci and Saccomandi, 2002); Y = Yeoh (Yeoh, 1990); C = Carroll (Carroll, 2011); O2 = Ogden (Ogden, 1972) with $M = 2$; YF = Yeoh–Fleming (Yeoh and Fleming, 1997).

other responsible for large strains. The specific nature of this model explains its better performance, which is accurate for both small and large strains.

In light of the above results, we selected the Yeoh–Fleming model for the deviatoric part W_d of the SED, which will be coupled with our proposed volumetric SED, W_h, in the next section. It is worth mentioning that there are many more incompressible strain energy functions for rubbers in the literature. The interested reader can refer to Dal et al. (2021) for a detailed review of isotropic hyperelastic constitutive models for rubber-like materials. In the present work, we only compared some of the most popular ones and chose the Yeoh–Fleming due to its accuracy in both moderate and large strains. It goes without saying that different formulations could be used. For instance, when dealing with soft tissues in problems of biomechanics, other hyperelastic models for W_d may be preferred (Madireddy et al., 2015; Puglisi and Saccomandi, 2016).

7. Combined SED and final results

In Section 5, a new formulation for the volumetric part W_h of the SED was proposed. This was done by analyzing independently the volumetric response of rubbers. In Section 6, a deviatoric part W_d of the SED was selected among the most popular in the literature. In particular, the Yeoh–Fleming model was found to be the most suitable. The analysis was done by assuming material incompressibility, with the sole purpose of investigating the shape-changing deformations of rubbers.

In the present section, the above deviatoric and volumetric parts W_d and W_h are combined. The resulting SED gives the complete description of both shape and volume deformations of rubbers.

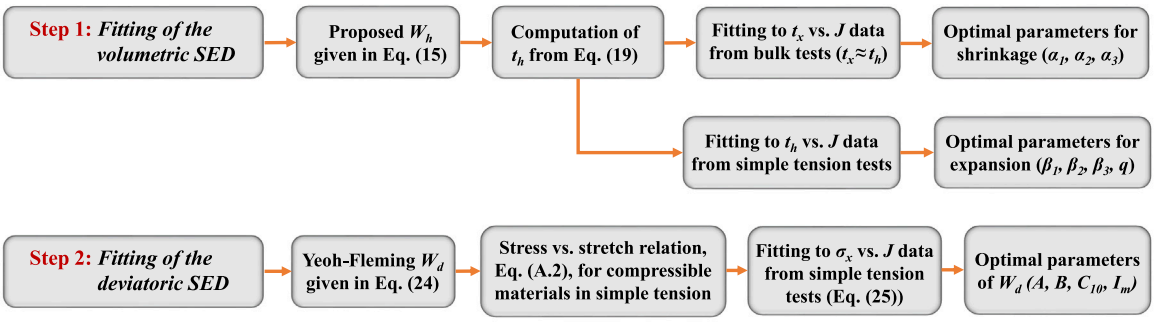

Fig. 12. Summary of the steps for fitting the parameters of volumetric and deviatoric parts of the combined SED proposed in this work.

7.1. The combined SED formulation

According to the deviatoric–volumetric decomposition of the SED, the Yeoh–Fleming model is written as a function of the first deviatoric strain invariant as

$$W_d\left(\bar{I}_1\right) = \frac{A}{B}\left(I_m - 3\right)\left(1 - e^{-B(\bar{I}_1-3)/(I_m-3)}\right) - C_{10}\left(I_m - 3\right)\ln\left(1 - \frac{\bar{I}_1 - 3}{I_m - 3}\right), \tag{24}$$

where $\bar{I}_1$ is defined in Eq. (7). The expression of the proposed volumetric SED, W_h, is reported in Eq. (15). The combined SED is obtained by summing the two contributions: $W = W_d\left(\bar{I}_1\right) + W_h(J)$.

The equilibrium solution in simple tension is expressed by Eqs. (A.1) and (A.2). The first is an implicit equation that allows us to compute numerically the lateral stretch λ_y as a function of longitudinal stretch λ_x. The second equation gives the expression of nominal stress σ_x as a function of longitudinal stretch λ_x. The derivatives $\partial W/\partial I_j$, with $j = 1, 2, 3$, are computed by applying the chain rule.

The equilibrium solution for the bulk test is expressed by Eqs. (A.5) and (A.6), which give closed-form expressions of the longitudinal and lateral stress components as a function of the volumetric change J. We recall that for the bulk test on rubbers, we have that $t_x \approx t_h$. In fact, in Section 5, the fitting parameters of the proposed function W_h were calibrated by using such an approximation. However, in the present section, since we are coupling deviatoric and volumetric contributions we are able to compute stress t_x by using the exact solution from Eq. (A.5).

Before proceeding to the discussion of the results of the combined formulation, we must point out an important fact. Thanks to the split of the energy function, the calibration of the fitting parameters for the volumetric part of the SED is entirely independent of the deviatoric contribution. In fact, the hydrostatic stress t_h depends only on W_h. However, since in finite elasticity a shape-changing deformation always implies a volume change, the same rule does not apply to the deviatoric part of the SED. The calibration of its parameters in simple tension requires the computation of stress σ_x (or t_x), which depends on both W_d and W_h. Hence, firstly the parameters of W_h are calibrated from bulk or hydrostatic tests. Then, the parameters of W_d are calibrated by fitting to experimental data the solution for compressible materials in simple tension. We recall that, in the previous section, the hypothesis of incompressibility was adopted only to select the most suitable deviatoric SED, not to obtain a definitive set of fitting parameters for the material model.

Based on the above, when dealing with compressible materials, volume changes have an effect on the response and the parameters of W_d must be calibrated after calibration of the parameters of W_h. Thus, our combined SED requires the calibration of the Yeoh–Fleming model parameters, which is presented in the following. The parameters of the proposed volumetric SED were already calibrated in Section 5 and are given in Table B.5. The overall procedure for parameter fitting is summarized in the scheme shown in Fig. 12.

7.2. Fitting of the Yeoh–Fleming deviatoric SED

The fitting process was performed using MATLAB. The experimental data from simple tension tests were imported as stress σ_{x_i} and stretch λ_{x_i}, where $i = 1, \ldots, n$ and n is the number of experimental data points. The constitutive parameters of the Yeoh–Fleming model were gathered in the parameter vector $\mathbf{p} = [A, B, C_{10}, I_m]$. The equilibrium equations in simple tension, expressed by Eqs. (A.1) and (A.2), were implemented in a MATLAB function. The implicit Eq. (A.1) was solved using *fsolve* to obtain for all data λ_{x_i} the corresponding values of lateral stretch $\lambda_{y_i}(\mathbf{p})$. The obtained values $\lambda_{y_i}(\mathbf{p})$ were inserted in Eq. (A.2) to compute the stress function $\sigma_x\left(\lambda_{x_i}, \lambda_{y_i}(\mathbf{p}), \mathbf{p}\right)$. Then, the following objective function was defined:

$$\mathrm{obj}(\mathbf{p}) = \sqrt{\sum_i^n \left(\sigma_x\left(\lambda_{x_i}, \lambda_{y_i}(\mathbf{p}), \mathbf{p}\right) - \sigma_{x_i}\right)^2}. \tag{25}$$

Hence, the optimal parameters are those that minimize the sum of squared residuals between analytical and experimental stress vs. stretch curves.

The minimization of Eq. (25) was carried out using function *fmincon*. The initial guess for the parameter vector was $\mathbf{p}_0 = [0.5, 0.01, 1, 2]$. The lower and upper bounds for the parameters were defined respectively as $\mathbf{p}_l = [0, 0, 0, 0]$ and $\mathbf{p}_u = [10, 1, 10, 20]$. The optimal parameters obtained from the optimization are reported in Table B.7. The equilibrium solutions for bulk and simple tension tests were computed with the optimal parameters and the final results for each rubber are shown in Fig. 13.

The plots in the left column of Fig. 13 show the t_x vs. J curves for $J < 1$ in comparison with the experimental data from bulk tests. We recall that, for the bulk tests, the calibration of the parameters of W_h was done under the approximation $t_x \approx t_h$ (see Fig. 7). Since now we combined both volumetric and deviatoric contributions, the exact solution was computed from Eq. (A.5) in terms of t_x vs. J relation. The above plots show that the model is accurate and confirm that for bulk tests there is no substantial difference between t_x and t_h. This provides further confirmation of such an approximation in the case of rubber-like materials.

The plots in the middle and right columns of Fig. 13 show respectively the σ_x vs. λ_x and λ_y vs. λ_x curves in comparison with the experimental data from simple tension tests. The results were computed by solving numerically the system composed of Eqs. (A.1) and (A.2). The model describes accurately the response in simple tension of all four rubbers considered.

8. Concluding remarks

The mechanical behavior of elastomers is typically studied under the hypothesis of material incompressibility. In this work, we presented experiments that show that this assumption may not be accurate for large deformations. We performed simple tension and bulk tests on four kinds of rubbers. During simple tension tests, we monitored both longitudinal and lateral displacements through digital image correlation. For small stretches, all the rubbers resulted nearly incompressible. As the longitudinal stretch increased, volume expansion up to 60% were observed in some rubbers. During bulk tests, an applied stress of 300 MPa produced volume shrinkage around $10-15\%$ for all the specimens. Combining the data from simple tension and bulk tests, a complete description of the volumetric response of the rubbers was obtained.

The volumetric SED formulations available in the literature failed to provide an accurate simulation of the response obtained from the above experiments, especially in the transition from small to moderate/large volume changes. The limitations of the available theories derive from the fact that they were developed mainly for foams and hydrogels. Compared to these materials, elastomers exhibit pronounced strain stiffening and softening for relatively small volume variations, resulting in a volumetric response that is in general different.

In light of the above, we proposed a novel volumetric SED. The proposed formulation counts for seven parameters in addition to the bulk modulus. Its advantages are:

- Accurate description of the response of elastomers for both small and large volume changes.
- Combination of two different response functions that allow predicting the two diverse responses of rubbers in shrinkage and expansion.
- For other compressible materials with different behaviors, the response functions can be easily replaced by other expressions.
- Possibility of a smooth transition between $J < 1$ and $J > 1$ using a sigmoid function to overcome numerical issues in the implementation in finite element codes.

Some popular incompressible strain energy functions were considered for modeling the shape-changing deformations of rubbers. After a comparison of their performance, the Yeoh–Fleming formulation was selected for the deviatoric part W_d of the SED. According to the deviatoric–volumetric split, the deviatoric part was combined with our proposed volumetric part W_h to obtain the final combined SED.

The equilibrium solutions for compressible materials were presented and a final fitting of the combined SED formulation to the experimental data was performed. The deviatoric–volumetric split allowed performing the fitting in two steps: (1) calibration of the parameters of W_h by fitting $t_h = dW_h/dJ$ to the experimental t_h vs. J data; (2) calibration of the parameters of W_d by fitting the equilibrium solution in simple tension to the experimental σ_x vs. λ_x data. The proposed model gave accurate descriptions of both shape deformations and volume changes of the elastomers considered. As far as the authors know, a comprehensive fitting of both deviatoric and volumetric contributions to experimental data involving large shrinkage and expansion had not yet been presented.

The proposed SED is useful to include the effect of volumetric deformations in nonlinear models for elastomers subjected to various stress states of practical interest. The function proposed may find applications also in biomechanics when dealing with soft tissues such as the brain, skin and arteries. Future works may focus on experimental tests involving biaxial stress states and on the implementation of the proposed SED in finite element codes.

Declaration of competing interest

The authors declare that they have no known competing financial interests or personal relationships that could have appeared to influence the work reported in this paper.

Data availability

Data will be made available on request.

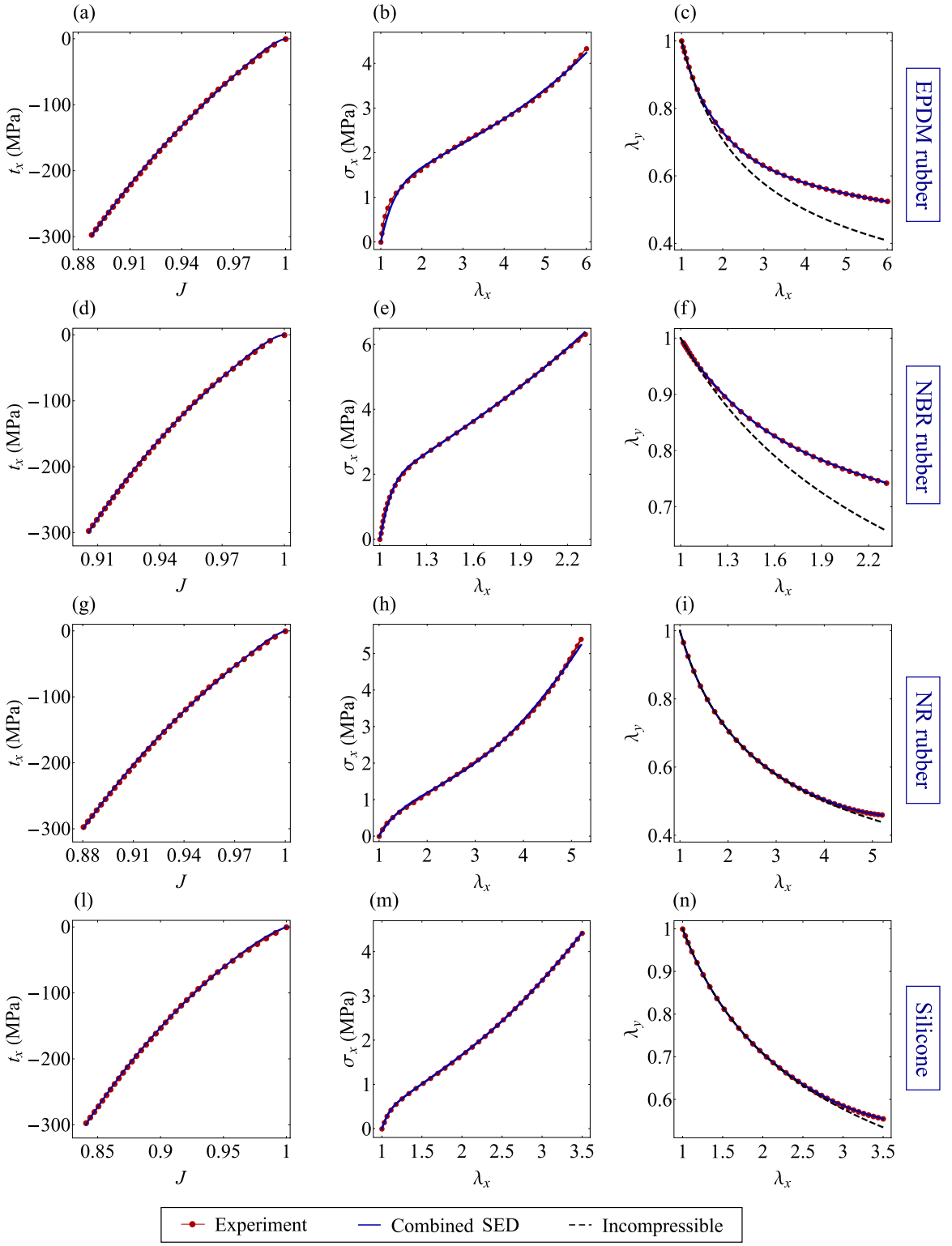

Fig. 13. Results of the combined SED formulation, composed of the Yeoh–Fleming model for the deviatoric part and the proposed function for the volumetric part. The results are shown for (a)–(c) EPDM, (d)–(f) NBR, (g)–(i) NR and (l)–(n) silicone. The t_x vs. J experimental data come from the bulk tests, while the σ_x vs. λ_x and λ_y vs. λ_x from the simple tension tests.

Acknowledgments

This work was supported by the Italian Ministry of University and Research (MUR) through research grant PRIN 2020 No. 2020EBLPLS on "Opportunities and challenges of nanotechnology in advanced and green construction materials". Financial support from the University of Modena and Reggio Emilia, Italy in the framework of "FAR Dipartimentale 2021–2022" (CUP E92F20000640001) is gratefully acknowledged. Support by the National Group of Mathematical Physics (GNFM-INdAM), Italy is also acknowledged. The authors would like to thank Mr. Ivano Lanzoni, who built the experimental device for bulk tests according to our specifications.

Appendix A. Equilibrium solutions for compressible and incompressible materials

In this appendix, we briefly summarize the solutions to the equilibrium problems considered in the present work: simple tension and bulk test.

A.1. Simple tension

We consider a homogeneous, isotropic and hyperelastic solid described by a stored energy function $W(I_1, I_2, I_3)$. We introduce the reference system x, y, z, where x is the longitudinal axis of the sample. In simple tension, uniaxial tractions are uniformly distributed on the basis of the solid and act in the x direction. We indicate the nominal stresses as σ_i and the true stresses as t_i, with $i = x, y, z$. In this case, the two lateral principal stresses are identically zero ($\sigma_y = \sigma_z = 0$). As a consequence of isotropy, the lateral stretches are equal to each other ($\lambda_y = \lambda_z$).

The equilibrium solution for a compressible hyperelastic solid under simple tension is given by (Lanzoni and Tarantino, 2015)

$$\frac{\partial W}{\partial I_1} + \left(\lambda_x^2 + \lambda_y^2\right)\frac{\partial W}{\partial I_2} + \lambda_x^2\lambda_y^2\frac{\partial W}{\partial I_3} = 0, \tag{A.1}$$

$$\sigma_x = 2\lambda_x\left(\frac{\partial W}{\partial I_1} + 2\lambda_y^2\frac{\partial W}{\partial I_2} + \lambda_y^4\frac{\partial W}{\partial I_3}\right). \tag{A.2}$$

From the first implicit equation, the lateral stretch λ_y can be determined for a given longitudinal stretch λ_x. The nominal stress σ_x is computed from the second equation and the true stress can be derived as $t_x = \sigma_x/\lambda_y^2$.

For an incompressible material, the condition $J = 1$ gives the following relation between lateral and longitudinal stretches: $\lambda_y = 1/\sqrt{\lambda_x}$. The equilibrium solution obtained from Eq. (5) is

$$\sigma_x = 2\left(1 - \frac{1}{\lambda_x^3}\right)\left(\lambda_x\frac{\partial W}{\partial I_1} + \frac{\partial W}{\partial I_2}\right). \tag{A.3}$$

In case of strain energy written as a function of the principal stretches, $W = \tilde{W}\left(\lambda_1, \lambda_2, \lambda_3\right)$, the nominal stresses for an incompressible material are computed as $\sigma_i = \partial\tilde{W}/\partial\lambda_i - p\lambda_i^{-1}$, with $i = 1, 2, 3$. In simple tension we have that $\tilde{W}\left(\lambda_x, 1/\sqrt{\lambda_x}, 1/\sqrt{\lambda_x}\right) = \hat{W}\left(\lambda_x\right)$ and the equilibrium reduces to

$$\sigma_x = \frac{d\hat{W}}{d\lambda_x}. \tag{A.4}$$

A.2. Bulk test

For the case of the bulk test, the lateral deformations are constrained, and thus $\lambda_y = \lambda_z = 1$ and $\lambda_x = J$. Using Eq. (3) along with the constraint on the lateral deformation, the following equilibrium solution is derived:

$$\sigma_x = t_x = 2J\left(\frac{\partial W}{\partial I_1} + 2\frac{\partial W}{\partial I_2} + \frac{\partial W}{\partial I_3}\right), \tag{A.5}$$

$$\sigma_y = 2\frac{\partial W}{\partial I_1} + 2\left(1 + J^2\right)\frac{\partial W}{\partial I_2} + 2J^2\frac{\partial W}{\partial I_3}. \tag{A.6}$$

Making explicit the deviatoric and volumetric parts of the energy function, $W = W_d(\bar{I}_1, \bar{I}_2) + W_h(J)$, Eq. (A.5) is written as follows

$$t_x = 2J\left(\frac{\partial W_d}{\partial I_1} + 2\frac{\partial W_d}{\partial I_2} + \frac{\partial W_d}{\partial I_3}\right) + \frac{dW_h}{dJ}. \tag{A.7}$$

The first and second addends are respectively the deviatoric and volumetric contributions to the stress t_x in the bulk test. In the following, we show that for rubber-like materials the deviatoric contribution, named t_d for convenience, can be neglected.

Recalling the definition of the deviatoric strain invariants given in Eq. (7) and using the chain rule to compute the derivatives, the first addend of Eq. (A.7) becomes

$$t_d = \frac{4}{3}\left(\frac{\partial W_d}{\partial \bar{I}_1}J^{2/3} + \frac{\partial W_d}{\partial \bar{I}_2}\right)\left(J^2 - 1\right)J^{-7/3}. \tag{A.8}$$

Table B.4
Parameters obtained by fitting the current volumetric SED formulations to the experimental data in Fig. 5. If applicable, the units are in MPa.

Formulation	EPDM		NBR		NR		Silicone	
	$J<1$	$J\geq 1$	$J<1$	$J\geq 1$	$J<1$	$J\geq 1$	$J<1$	$J\geq 1$
Doll (Doll and Schweizerhof, 2000)	$\alpha=0.01$ $\beta=25.25$	$\alpha=3.46$ $\beta=517.12$	$\alpha=0.01$ $\beta=35.58$	$\alpha=5.67$ $\beta=395.96$	$\alpha=0.01$ $\beta=18.86$	$\alpha=9.91$ $\beta=172.44$	$\alpha=0.01$ $\beta=9.97$	$\alpha=12.77$ $\beta=331.77$
Montella (Montella et al., 2016)	$\kappa_2=160750$ $\beta_1=0.125$ $\beta_2=0.125$ $m=4$	$\kappa_2=6.02$ $\beta_1=0.125$ $\beta_2=5.01$ $m=22.44$	$\kappa_2=302305$ $\beta_1=0.125$ $\beta_2=0.125$ $m=4$	$\kappa_2=11.8$ $\beta_1=0.125$ $\beta_2=4.17$ $m=14.15$	$\kappa_2=113343$ $\beta_1=0.125$ $\beta_2=0.125$ $m=4$	$\kappa_2=17.93$ $\beta_1=0.125$ $\beta_2=7.34$ $m=10.61$	$\kappa_2=31223$ $\beta_1=0.125$ $\beta_2=0.125$ $m=4$	$\kappa_2=15.18$ $\beta_1=0.125$ $\beta_2=7.53$ $m=9.95$
Moerman (Moerman et al., 2020)	$J_2=0.881$ $s_2=0.194$ $q_2=0$	$J_1=2.85$ $s_1=0.585$ $q_1=0.987$	$J_2=0.902$ $s_2=0.095$ $q_2=0$	$J_1=9.982$ $s_1=0.721$ $q_1=0.972$	$J_2=0.869$ $s_2=0.098$ $q_2=0$	$J_1=9.99$ $s_1=2.69$ $q_1=0.891$	$J_2=0.816$ $s_2=0.1$ $q_2=0$	$J_1=9.55$ $s_1=1.65$ $q_1=0.931$

Convexity of the stored energy function requires that $\partial W_d/\partial \bar{I}_1 > 0$ and $\partial W_d/\partial \bar{I}_2 > 0$ (Ciarlet, 1988). Therefore, since in the bulk test $J \leq 1$, we have that

$$|t_d| \leq \left| \frac{4}{3}\left(\frac{\partial W_d}{\partial \bar{I}_1} + \frac{\partial W_d}{\partial \bar{I}_2}\right)\left(J^2-1\right)J^{-7/3} \right|. \tag{A.9}$$

We recall that the equilibrium solution in simple shear for incompressible materials (Horgan and Murphy, 2010) is $t_{12} = \tilde{\mu}\,\gamma$, being γ the amount of shear, t_{12} the Cauchy shear stress and $\tilde{\mu} = 2\left(\partial W_d/\partial \bar{I}_1 + \partial W_d/\partial \bar{I}_2\right)$. The quantity $\tilde{\mu}$ tends to the infinitesimal shear modulus μ in the range of small strains and can be interpreted as a secant shear modulus in nonlinear elasticity. Eq. (A.9) is rewritten as

$$|t_d| \leq \frac{2\,(J+1)}{3J^{7/3}}\tilde{\mu}\,|(J-1)|\,. \tag{A.10}$$

Regarding the volumetric contribution $t_h = dW_h/dJ$, we introduce the secant bulk modulus $\tilde{\kappa}$ and write

$$|t_h| = \tilde{\kappa}\,|(J-1)|\,. \tag{A.11}$$

The experiments carried out in the present work and others (see, e.g., Adams and Gibson, 1930; Wood and Martin, 1964; Bridgman, 1945; Boyce and Arruda, 2000) show that elastomers exhibit a hardening trend during volume shrinkage. Namely, the secant bulk modulus in shrinkage is initially equal to κ and then increases as J decreases. From Eqs. (A.10) and (A.11) we conclude the following:

$$\frac{t_d}{t_h} \leq \frac{2\,(J+1)}{3J^{7/3}}\frac{\tilde{\mu}}{\tilde{\kappa}}. \tag{A.12}$$

The multiplying factor $2(J+1)/(3J^{7/3})$ increases as J decreases. However, in the bulk test, the J values of interest for rubbers are between 0.8 and 1. This range covers widely the values of pressure applied in real applications. When $J<0.8$ the applied pressure becomes extremely large and, from a practical point of view, this is of no interest.[2] With that said, the value of the multiplying factor for $J=0.8$ is very close to 2. Hence, in the range $J\in[0.8,1]$ we have that

$$\frac{t_d}{t_h} \leq \frac{2\tilde{\mu}}{\tilde{\kappa}}. \tag{A.13}$$

For rubber-like materials $\tilde{\mu} \ll \tilde{\kappa}$ and therefore the deviatoric contribution t_d to the stress t_x in the bulk test can be neglected. Hence, from Eq. (A.7) we obtain

$$\sigma_x = t_x \approx \frac{dW_h}{dJ}. \tag{A.14}$$

It is worth mentioning that Horgan and Murphy (2009a) obtained the same result, but considering nearly incompressible elastomers. They reported that for infinitesimal volume changes t_d is approximated by the linearization $\beta\,(J-1)$, where β is a constant of the order of μ. Since dW_h/dJ is approximated by $\kappa\,(J-1)$ and $\mu \ll \kappa$, the deviatoric contribution can be neglected and Eq. (A.14) is obtained. We demonstrated that this result remains valid even when dealing with large volumetric deformations.

Appendix B. Fitting parameters

Tables B.4, B.5, B.6 and B.7 present respectively the parameters obtained from the fitting described in Sections 4.2, 5.2, 6.2 and 7.2.

[2] For instance, Bridgman (1945) observed volume shrinkage of 20%–25% on various rubbers with an applied pressure of around 2.5 GPa.

Table B.5
Parameters obtained by fitting the proposed volumetric SED to the experimental data in Fig. 5.

Formulation	EPDM	NBR	NR	Silicone
Proposed SED, Eq. (15)	$\alpha_1 = 81.07$ $\alpha_2 = 5.1$ $\alpha_3 = 84.80$ $\beta_1 = 2.23$ $\beta_2 = 9.05$ $\beta_3 = 6.88 \times 10^{-4}$ $q = 0.974$	$\alpha_1 = 83.33$ $\alpha_2 = 8.03$ $\alpha_3 = 89.69$ $\beta_1 = 4.18$ $\beta_2 = 14.03$ $\beta_3 = 13.76 \times 10^{-4}$ $q = 0.953$	$\alpha_1 = 92.59$ $\alpha_2 = 4.99$ $\alpha_3 = 95.47$ $\beta_1 = 7.09$ $\beta_2 = 69.25$ $\beta_3 = 13.14 \times 10^{-4}$ $q = 0.723$	$\alpha_1 = 32.26$ $\alpha_2 = 4.51$ $\alpha_3 = 34.12$ $\beta_1 = 5.03$ $\beta_2 = 68.86$ $\beta_3 = 1 \times 10^{-4}$ $q = 0.461$

Table B.6
Parameters obtained by fitting the current deviatoric SED formulations to the experimental data in simple tension. If applicable, the units are in MPa.

Formulation	EPDM	NBR	NR	Silicone
Gent (Gent, 1996)	$\mu = 0.68$ $J_m = 198$	$\mu = 3.08$ $J_m = 145$	$\mu = 0.63$ $J_m = 61.64$	$\mu = 0.91$ $J_m = 32.52$
Gent-Gent (Pucci and Saccomandi, 2002)	$C_1 = 0.28$ $C_2 = 1.68$ $J_m = 202.3$	$C_1 = 0.55$ $C_2 = 5.43$ $J_m = 6.78$	$C_1 = 0.30$ $C_2 = 0.22$ $J_m = 57.61$	$C_1 = 0.44$ $C_2 = 0.16$ $J_m = 29.89$
Yeoh (Yeoh, 1990)	$C_{10} = 0.01$ $C_{20} = 0.09$ $C_{30} = -9.1 \times 10^{-6}$	$C_{10} = 0.01$ $C_{20} = 0.35$ $C_{30} = -1.76 \times 10^{-4}$	$C_{10} = 0.19$ $C_{20} = 0.033$ $C_{30} = 8.89 \times 10^{-5}$	$C_{10} = 0.29$ $C_{20} = 0.04$ $C_{30} = 4.34 \times 10^{-4}$
Carroll (Carroll, 2011)	$A = 0.27$ $B = 2.84 \times 10^{-7}$ $C = 1.74$	$A = 0.12$ $B = 6.82 \times 10^{-4}$ $C = 7.85$	$A = 0.37$ $B = 2.10 \times 10^{-6}$ $C = -0.26$	$A = 0.52$ $B = 1.91 \times 10^{-5}$ $C = -0.28$
Ogden (Ogden, 1972)	$\mu_1 = 2.62$ $\mu_2 = 0.26$ $\alpha_1 = 3.1 \times 10^{-3}$ $\alpha_2 = 2.99$	$\mu_1 = 0.017$ $\mu_2 = 8.49$ $\alpha_1 = 9.26$ $\alpha_2 = 0.011$	$\mu_1 = 1.4$ $\mu_2 = 0.02$ $\alpha_1 = 1.75$ $\alpha_2 = 4.94$	$\mu_1 = 0.6$ $\mu_2 = 1.49$ $\alpha_1 = 3.43$ $\alpha_2 = 1.1 \times 10^{-3}$
Yeoh–Fleming (Yeoh and Fleming, 1997)	$A = 0.29$ $B = 7 \times 10^{-3}$ $C_{10} = 0.44$ $I_m = 1.49$	$A = 1.28$ $B = 2.16 \times 10^{-3}$ $C_{10} = 2.74$ $I_m = 2.94$	$A = 0.27$ $B = 0.078$ $C_{10} = 0.09$ $I_m = 0.02$	$A = 0.43$ $B = 1.72 \times 10^{-3}$ $C_{10} = 0.49$ $I_m = 2.96$

Table B.7
Parameters obtained by fitting the combined formulation to the experimental data. The deviatoric part W_d of the SED is expressed by the Yeoh–Fleming model (Yeoh and Fleming, 1997), while the volumetric part W_h is defined by the function proposed in the present work, given in Eq. (15). The calibrated parameters of W_h are those reported in Table B.5 and are repeated here for the convenience of the reader. If applicable, the units are in MPa.

Combined formulation	EPDM	NBR	NR	Silicone
W_d	$A = 0.313$ $B = 0.03$ $C_{10} = 0.373$ $I_m = 1.3$	$A = 1.31$ $B = 7.82 \times 10^{-3}$ $C_{10} = 2.59$ $I_m = 2.93$	$A = 0.258$ $B = 0.074$ $C_{10} = 0.121$ $I_m = 0.628$	$A = 0.417$ $B = 4.32 \times 10^{-3}$ $C_{10} = 0.397$ $I_m = 2.92$
W_h	$\alpha_1 = 81.07$ $\alpha_2 = 5.1$ $\alpha_3 = 84.80$ $\beta_1 = 2.23$ $\beta_2 = 9.05$ $\beta_3 = 6.88 \times 10^{-4}$ $q = 0.974$	$\alpha_1 = 83.33$ $\alpha_2 = 8.03$ $\alpha_3 = 89.69$ $\beta_1 = 4.18$ $\beta_2 = 14.03$ $\beta_3 = 13.76 \times 10^{-4}$ $q = 0.953$	$\alpha_1 = 92.59$ $\alpha_2 = 4.99$ $\alpha_3 = 95.47$ $\beta_1 = 7.09$ $\beta_2 = 69.25$ $\beta_3 = 13.14 \times 10^{-4}$ $q = 0.723$	$\alpha_1 = 32.26$ $\alpha_2 = 4.51$ $\alpha_3 = 34.12$ $\beta_1 = 5.03$ $\beta_2 = 68.86$ $\beta_3 = 1 \times 10^{-4}$ $q = 0.461$

Appendix C. Smooth approximation of the Heaviside step function

For the purpose of a numerical implementation of the proposed volumetric SED, it may be desirable to approximate the Heaviside step function with a smooth continuous function. We propose the following smooth approximation

$$H(1-J) \approx \frac{1-\tanh\left(10^3\,(J-1)\right)}{2} = \rho_c, \quad H(J-1) \approx \frac{1+\tanh\left(10^3\,(J-1)\right)}{2} = \rho_t. \tag{C.1}$$

The factor 10^3 ensures an adequate steepness of functions ρ_c and ρ_t when $J \to 1$. With this substitution, the volumetric strain energy and the hydrostatic stress become

$$W_h(J) = \kappa \int \left(\rho_c \psi_c + \rho_t \psi_t\right) dJ, \tag{C.2}$$

$$t_h(J) = \kappa\left(\rho_c \psi_c + \rho_t \psi_t\right). \tag{C.3}$$

For a detailed discussion on smooth approximations of step functions, the reader is referred to Iliev et al. (2017), Alyukov (2011) and Markov et al. (2018).

Appendix D. Mathematical requirements for the proposed volumetric SED

In this appendix, we investigate the requirements that the parameters of the proposed volumetric SED must fulfill for the physical plausibility of the model. For the sake of clarity, we recall that the proposed formulation is

$$W_h(J) = \kappa\left[H(1-J)\Psi_c + H(J-1)\Psi_t\right], \tag{D.1}$$

where H is the Heaviside step function defined in Eq. (16), and Ψ_c and Ψ_t are

$$\Psi_c(J) = \frac{1}{\alpha_1+\alpha_2-\alpha_3}\left[\left(J + \frac{J^{\alpha_1+1}}{\alpha_1+1} + \frac{J^{-(\alpha_2-1)}}{\alpha_2-1} - \frac{J^{\alpha_3+1}}{\alpha_3+1}\right) - \left(1 + \frac{1}{\alpha_1+1} + \frac{1}{\alpha_2-1} - \frac{1}{\alpha_3+1}\right)\right], \tag{D.2}$$

$$\Psi_t(J) = (1-q)\left[\frac{\beta_2 e^{\beta_1(J-1)} + \beta_1 e^{-\beta_2(J-1)}}{\beta_1\beta_2(\beta_1+\beta_2)} - \frac{1}{\beta_1\beta_2}\right] + q\beta_3^2 \ln\left(\cosh\left(\frac{J-1}{\beta_3}\right)\right). \tag{D.3}$$

The hydrostatic stress is computed as

$$t_h(J) = \frac{dW_h(J)}{dJ} = \kappa\left[H(1-J)\psi_c + H(J-1)\psi_t\right] \tag{D.4}$$

where

$$\psi_c(J) = \frac{d\Psi_c(J)}{dJ} = \frac{1 + J^{\alpha_1} - J^{-\alpha_2} - J^{\alpha_3}}{\alpha_1+\alpha_2-\alpha_3}, \tag{D.5}$$

$$\psi_t(J) = \frac{d\Psi_t(J)}{dJ} = (1-q)\frac{e^{\beta_1(J-1)} - e^{-\beta_2(J-1)}}{\beta_1+\beta_2} + q\beta_3 \tanh\left(\frac{J-1}{\beta_3}\right). \tag{D.6}$$

The tangent modulus is computed as the second derivative of the energy with respect to J, namely

$$\frac{d^2W_h(J)}{dJ^2} = \kappa\left[H(1-J)\frac{d\psi_c}{dJ} + H(J-1)\frac{d\psi_t}{dJ}\right]. \tag{D.7}$$

For volume shrinkage ($J < 1$) the tangent modulus reduces to

$$\frac{d^2W_h(J)}{dJ^2} = \kappa\frac{d\psi_c(J)}{dJ} = \kappa\frac{\alpha_1 J^{\alpha_1-1} + \alpha_2 J^{-\alpha_2-1} - \alpha_3 J^{\alpha_3-1}}{\alpha_1+\alpha_2-\alpha_3}, \tag{D.8}$$

whereas for volume expansion ($J > 1$) its expression is

$$\frac{d^2W_h(J)}{dJ^2} = \kappa\frac{d\psi_t(J)}{dJ} = \kappa\left[(1-q)\frac{\beta_1 e^{\beta_1(J-1)} + \beta_2 e^{-\beta_2(J-1)}}{\beta_1+\beta_2} + q\,\mathrm{sech}^2\left(\frac{J-1}{\beta_3}\right)\right]. \tag{D.9}$$

The ten criteria for physical plausibility are reported in Table 1 of the work by Moerman et al. (2020). Criteria I and II impose that the energy and the stress must vanish in the reference state ($J = 1$). These conditions are satisfied because Eqs. (D.1) and (D.4) evaluated for $J = 1$ give $W_h(1) = 0$ and $t_h(1) = 0$. Criterion III requires the energy to be positive in the entire J domain. Provided that $\min W_h(J) = W_h(1) = 0$, the above condition is ensured by verifying the convexity of W_h, which will be discussed in the following (criterion IX). Criterion IV states that the tangent modulus d^2W_h/dJ^2 computed for $J = 1$ must be equal to the bulk modulus κ, for consistency with linear elasticity. Eq. (D.7) evaluated in $J = 1$ satisfies this requirement.

Criteria V, VI, VII and VIII impose conditions on the behaviors of W_h and t_h for $J \to 0$ and $J \to +\infty$. We remark that the Heaviside step function allows to decouple the responses in shrinkage and expansion. Therefore, it is sufficient to study the functions Ψ_c, ψ_c, Ψ_t and ψ_t to determine the behaviors of W_h and t_h at the boundaries of the domain. To ensure that an infinite energy is required to reduce to zero the volume of a solid (criterion V), the following limit must be satisfied:

$$\lim_{J\to 0} \Psi_c(J) = +\infty, \tag{D.10}$$

with Ψ_c expressed by Eq. (D.2). This happens with the following conditions on α_1, α_2 and α_3:

$$\begin{cases} \alpha_1 > -1,\ \alpha_1+\alpha_2-\alpha_3 > 0 \\ \alpha_2 > 1,\ \alpha_3 \neq -1 \quad \text{or} \quad \alpha_3 < -1,\ \alpha_2 \neq 1 \end{cases} \tag{D.11}$$

The energy remains unchanged when parameters α_2 and α_3 are swapped and changed in sign. Thus, the case $\alpha_3 < -1,\ \alpha_2 \neq 1$ is equivalent to the case $\alpha_2 > 1,\ \alpha_3 \neq -1$ and describes the same behavior. Therefore we only consider the condition $\alpha_2 > 1,\ \alpha_3 \neq -1$. An infinite negative stress is necessary to reduce the volume to zero (criterion VI), namely

$$\lim_{J\to 0} \psi_c(J) = -\infty, \tag{D.12}$$

with ψ_c given by Eq. (D.5). The following conditions are necessary to fulfill the above equation:

$$\begin{cases} \alpha_1 > 0, \ \alpha_1 + \alpha_2 - \alpha_3 > 0 \\ \alpha_2 > 0 \quad \text{or} \quad \alpha_3 < 0 \end{cases} \tag{D.13}$$

Similarly to the energy, the hydrostatic stress remains unchanged when α_2 and α_3 are swapped and changed in sign. Hence, condition $\alpha_2 > 0$ is equivalent to condition $\alpha_3 < 0$, thus we limit to the case $\alpha_2 > 0$. In addition, from a mathematical standpoint when $\alpha_2 > 0$ parameter α_3 can assume any real value. However, if $\alpha_3 < 0$ the term $-J^{\alpha_3}$ behaves the same as $-J^{-\alpha_2}$ and goes to infinity when $J \to 0$. As explained in Section 5.1, we are instead interested in a term that contributes to the variation of stiffness in the region of small to moderate shrinkage, without affecting the response for large shrinkage. This behavior is obtained assuming $\alpha_3 > 0$, therefore we restrict our attention to this case. Considering the restrictions on both energy and stress, the overall constraints in shrinkage are

$$\alpha_1 > 0, \ \alpha_2 > 1, \ \alpha_3 > 0, \ \alpha_1 + \alpha_2 - \alpha_3 > 0. \tag{D.14}$$

An infinite energy is required to infinitely expand the volume of a solid (criterion VII), therefore

$$\lim_{J \to +\infty} \Psi_t(J) = +\infty, \tag{D.15}$$

with Ψ_t expressed by Eq. (D.3). Parameter q has the boundaries $0 \leq q < 1$. In addition, the functions involved with parameter β_3 are even, thus we consider only $\beta_3 > 0$. The above limit is satisfied if $\beta_1 > 0$ and $\beta_2 > 0$, or $\beta_1 < 0$ and $\beta_2 < 0$, or $\beta_1 < 0$ and $\beta_2 > 0$. When β_1 and β_2 have the same sign, function Ψ_t does not vary if they are both positive or negative. Thus, we discard the case in which $\beta_1 < 0$ and $\beta_2 < 0$. Criterion VIII states that an infinite positive stress is necessary to infinitely expand a volume, thus

$$\lim_{J \to +\infty} \psi_t(J) = +\infty, \tag{D.16}$$

with ψ_t expressed by Eq. (D.6). This limit is satisfied if $\beta_1 > 0$ and $\beta_2 > 0$.

Criterion IX imposes the condition of polyconvexity of the volumetric part of the SED, namely the tangent modulus d^2W_h/dJ^2 must be positive in the entire domain. For $J > 1$, this is true if $\beta_1 > 0$ and $\beta_2 > 0$. For $J < 1$, the tangent modulus is always positive if $\alpha_1 + \alpha_2 - \alpha_3 > 0$. Finally, criterion X is guaranteed by the Heaviside step function (or its smooth approximation), which provides independent control of the responses in shrinkage and expansion.

In summary, the parameters of the proposed volumetric SED must satisfy the following constraints:

$$\begin{cases} \beta_1 > 0, \ \beta_2 > 0, \ \beta_3 > 0, \ 0 \leq q < 1 \\ \alpha_1 > 0, \ \alpha_2 > 1, \ \alpha_3 > 0, \ \alpha_1 + \alpha_2 - \alpha_3 > 0 \end{cases} \tag{D.17}$$

References

Adams, L.H., Gibson, R.E., 1930. The compressibility of rubber. Rubber Chem. Technol. 3 (4), 555–562.

Alyukov, S.V., 2011. Approximation of step functions in problems of mathematical modeling. Math. Models Comput. Simul. 3, 661–669.

Angeli, P., Russo, G., Paschini, A., 2013. Carbon fiber-reinforced rectangular isolators with compressible elastomer: Analytical solution for compression and bending. Int. J. Solids Struct. 50 (22–23), 3519–3527.

Armero, F., 2000. On the locking and stability of finite elements in finite deformation plane strain problems. Comput. Struct. 75 (3), 261–290.

Bardy, E., Mollendorf, J., Pendergast, D., 2005. Thermal conductivity and compressive strain of foam neoprene insulation under hydrostatic pressure. J. Phys. D: Appl. Phys. 38 (20), 3832.

Baschetti, M.G., Minelli, M., 2020. Test methods for the characterization of gas and vapor permeability in polymers for food packaging application: A review. Polym. Test. 89, 106606.

Bischoff, J.E., Arruda, E.M., Grosh, K., 2001. A new constitutive model for the compressibility of elastomers at finite deformations. Rubber Chem. Technol. 74 (4), 541–559.

Blaber, J., Adair, B., Antoniou, A., 2015. Ncorr: open-source 2D digital image correlation matlab software. Exp. Mech. 55 (6), 1105–1122.

Blatz, P.J., Ko, W.L., 1962. Application of finite elastic theory to the deformation of rubbery materials. Trans. Soc. Rheol. 6 (1), 223–252.

Boyce, M.C., Arruda, E.M., 2000. Constitutive models of rubber elasticity: a review. Rubber Chem. Technol. 73 (3), 504–523.

Bridgman, P.W., 1945. The compression of sixty-one solid substances to 25,000 kg/cm^2, determined by a new rapid method. In: Proc. Am. Acad. Arts Sci, Vol. 76, No. 9. p. 24.

Carroll, M.M., 2011. A strain energy function for vulcanized rubbers. J. Elasticity 103, 173–187.

Ciarlet, P.G., 1988. Mathematical Elasticity: Three-Dimensional Elasticity, Vol. I. North-Holland Publishing Co., Amsterdam.

Dal, H., Açıkgöz, K., Badienia, Y., 2021. On the performance of isotropic hyperelastic constitutive models for rubber-like materials: A state of the art review. Appl. Mech. Rev. 73 (2).

Destrade, M., Saccomandi, G., Sgura, I., 2017. Methodical fitting for mathematical models of rubber-like materials. Proc. R. Soc. A 473 (2198), 20160811.

Doll, S., Schweizerhof, K., 2000. On the development of volumetric strain energy functions. J. Appl. Mech. 67 (1), 17–21.

Gent, A.N., 1996. A new constitutive relation for rubber. Rubber Chem. Technol. 69 (1), 59–61.

Gurvich, M.R., Fleischman, T.S., 2003. A simple approach to characterize finite compressibility of elastomers. Rubber Chem. Technol. 76 (4), 912–922.

Haines, D.W., Wilson, W.D., 1979. Strain-energy density function for rubberlike materials. J. Mech. Phys. Solids 27 (4), 345–360.

Heisserer, U., Hartmann, S., Düster, A., Yosibash, Z., 2008. On volumetric locking-free behaviour of p-version finite elements under finite deformations. Commun. Numer. Methods. Eng. 24 (11), 1019–1032.

Hencky, H., 1933. The elastic behavior of vulcanized rubber. Rubber Chem. Technol. 6 (2), 217–224.

Hill, R., 1979. Aspects of invariance in solid mechanics. Adv. Appl. Mech. 18, 1–75.

Horgan, C.O., 2015. The remarkable Gent constitutive model for hyperelastic materials. Int. J. Non-Linear Mech. 68, 9–16.

Horgan, C.O., Murphy, J.G., 2009a. Constitutive modeling for moderate deformations of slightly compressible rubber. J. Rheol. 53 (1), 153–168.

Horgan, C.O., Murphy, J.G., 2009b. On the volumetric part of strain-energy functions used in the constitutive modeling of slightly compressible solid rubbers. Int. J. Solids Struct. 46 (16), 3078–3085.
Horgan, C.O., Murphy, J.G., 2010. Simple shearing of incompressible and slightly compressible isotropic nonlinearly elastic materials. J. Elasticity 98, 205–221.
Horgan, C.O., Saccomandi, G., 2004. Constitutive models for compressible nonlinearly elastic materials with limiting chain extensibility. J. Elasticity 77, 123–138.
Iliev, A., Kyurkchiev, N., Markov, S., 2017. On the approximation of the step function by some sigmoid functions. Math. Comput. Simulation 133, 223–234.
Khajehsaeid, H., Arghavani, J., Naghdabadi, R., 2013. A hyperelastic constitutive model for rubber-like materials. Eur. J. Mech. A Solids 38, 144–151.
Kugler, H.P., Stacer, R.G., Steimle, C., 1990. Direct measurement of Poisson's ratio in elastomers. Rubber Chem. Technol. 63 (4), 473–487.
Landis, C.M., Huang, R., Hutchinson, J.W., 2022. Formation of surface wrinkles and creases in constrained dielectric elastomers subject to electromechanical loading. J. Mech. Phys. Solids 167, 105023.
Lanzoni, L., Tarantino, A.M., 2015. Equilibrium configurations and stability of a damaged body under uniaxial tractions. Z. Angew. Math. Phys. 66 (1), 171–190.
Lengyel, T.H., Qi, Y., Schiavone, P., Long, R., 2016. Interface crack between a compressible elastomer and a rigid substrate with finite slippage. J. Mech. Phys. Solids 90, 142–159.
Levinson, M., Burgess, I.W., 1971. A comparison of some simple constitutive relations for slightly compressible rubber-like materials. Int. J. Mech. Sci. 13 (6), 563–572.
Li, J., Mayau, D., Lagarrigue, V., 2008. A constitutive model dealing with damage due to cavity growth and the Mullins effect in rubber-like materials under triaxial loading. J. Mech. Phys. Solids 56 (3), 953–973.
Liang, Y.J., McQuien, J.S., Iarve, E.V., 2020. Implementation of the regularized extended finite element method in Abaqus framework for fracture modeling in laminated composites. Eng. Fract. Mech. 230, 106989.
Liu, X., Wang, L.Y., Zhao, L.F., He, H.F., Shao, X.Y., Fang, G.B., Wan, Z.G., Zeng, R.C., 2018. Research progress of graphene-based rubber nanocomposites. Polym. Compos. 39 (4), 1006–1022.
Loew, P.J., Peters, B., Beex, L.A., 2019. Rate-dependent phase-field damage modeling of rubber and its experimental parameter identification. J. Mech. Phys. Solids 127, 266–294.
Madireddy, S., Sista, B., Vemaganti, K., 2015. A Bayesian approach to selecting hyperelastic constitutive models of soft tissue. Comput. Methods Appl. Mech. Engrg. 291, 102–122.
Markov, S., Kyurkchiev, N., Iliev, A., Rahnev, A., 2018. On the approximation of the generalized cut functions of degree p+1 by smooth hyper-log-logistic function. Dynam. Systems Appl. 27 (4), 715–728.
Mihai, L.A., Goriely, A., 2017. How to characterize a nonlinear elastic material? A review on nonlinear constitutive parameters in isotropic finite elasticity. Proc. R. Soc. A 473 (2207), 20170607.
Moerman, K.M., Fereidoonnezhad, B., McGarry, J.P., 2020. Novel hyperelastic models for large volumetric deformations. Int. J. Solids Struct. 193, 474–491.
Montella, G., Govindjee, S., Neff, P., 2016. The exponentiated Hencky strain energy in modeling tire derived material for moderately large deformations. J. Eng. Mater. Technol. 138 (3), 031008.
Mott, P.H., Dorgan, J.R., Roland, C.M., 2008. The bulk modulus and Poisson's ratio of "incompressible" materials. J. Sound Vib. 312 (4–5), 572–575.
Neff, P., Lankeit, J., Ghiba, I.D., Martin, R., Steigmann, D., 2015. The exponentiated Hencky-logarithmic strain energy. Part II: coercivity, planar polyconvexity and existence of minimizers. Z. Angew. Math. Phys. 66, 1671–1693.
Ogden, R.W., 1972. Large deformation isotropic elasticity–on the correlation of theory and experiment for incompressible rubberlike solids. Proc. R. Soc. Lond. Ser. A Math. Phys. Eng. Sci. 326 (1567), 565–584.
Ogden, R.W., Saccomandi, G., Sgura, I., 2004. Fitting hyperelastic models to experimental data. Comput. Mech. 34, 484–502.
Omnès, B., Thuillier, S., Pilvin, P., Grohens, Y., Gillet, S., 2008. Effective properties of carbon black filled natural rubber: Experiments and modeling. Composites A 39 (7), 1141–1149.
Pelliciari, M., Sirotti, S., Aloisio, A., Tarantino, A.M., 2022. Analytical, numerical and experimental study of the finite inflation of circular membranes. Int. J. Mech. Sci. 226, 107383.
Pelliciari, M., Tarantino, A.M., 2022. A continuum model for circular graphene membranes under uniform lateral pressure. J. Elasticity 151 (2), 273–303.
Peng, X., Han, L., Li, L., 2021. A consistently compressible Mooney-Rivlin model for the vulcanized rubber based on the Penn's experimental data. Polym. Eng. Sci. 61 (9), 2287–2294.
Petre, M.T., Erdemir, A., Cavanagh, P.R., 2006. Determination of elastomeric foam parameters for simulations of complex loading. Comput. Methods Biomech. Biomed. Eng. 9 (4), 231–242.
Pucci, E., Saccomandi, G., 2002. A note on the Gent model for rubber-like materials. Rubber Chem. Technol. 75 (5), 839–852.
Puglisi, G., Saccomandi, G., 2016. Multi-scale modelling of rubber-like materials and soft tissues: an appraisal. Philos. Trans. R. Soc. Lond. Ser. A Math. Phys. Eng. Sci. 472 (2187), 20160060.
Rivlin, R.S., 1948. Large elastic deformations of isotropic materials IV. Further developments of the general theory. Philos. Trans. R. Soc. Lond. Ser. A Math. Phys. Sci. 241 (835), 379–397.
Rivlin, R.S., Saunders, D.W., 1997. Large Elastic Deformations of Isotropic Materials: VII. Experiments on the Deformation of Rubber. Springer.
Sansour, C., 2008. On the physical assumptions underlying the volumetric-isochoric split and the case of anisotropy. Eur. J. Mech. A Solids 27 (1), 28–39.
Sethulekshmi, A., Saritha, A., Joseph, K., 2022. A comprehensive review on the recent advancements in natural rubber nanocomposites. Int. J. Biol. Macromol. 194, 819–842.
Simo, J.C., 1988. A framework for finite strain elastoplasticity based on maximum plastic dissipation and the multiplicative decomposition: Part I. Continuum formulation. Comput. Methods Appl. Mech. Engrg. 66 (2), 199–219.
Singh, V., Racherla, V., 2022. Deformation behavior of fluid-filled porous elastomers: Analytical estimates and validation. J. Mech. Phys. Solids 163, 104835.
Sirotti, S., Pelliciari, M., Aloisio, A., Tarantino, A.M., 2023. Analytical pressure–deflection curves for the inflation of pre-stretched circular membranes. Eur. J. Mech. A Solids 97, 104831.
Starkova, O., Aniskevich, A., 2010. Poisson's ratio and the incompressibility relation for various strain measures with the example of a silica-filled SBR rubber in uniaxial tension tests. Polym. Test. 29 (3), 310–318.
Steck, D., Qu, J., Kordmahale, S.B., Tscharnuter, D., Muliana, A., Kameoka, J., 2019. Mechanical responses of Ecoflex silicone rubber: Compressible and incompressible behaviors. J. Appl. Polym. Sci. 136 (5), 47025.
Steinmann, P., Hossain, M., Possart, G., 2012. Hyperelastic models for rubber-like materials: consistent tangent operators and suitability for Treloar's data. Arch. Appl. Mech. 82, 1183–1217.
Treloar, L., 1943. The elasticity of a network of long-chain molecules–II. Trans. Faraday Soc. 39, 241–246.
Tsang, H.H., 2008. Seismic isolation by rubber–soil mixtures for developing countries. Earthq. Eng. Struct. Dyn. 37 (2), 283–303.
Upadhyay, K., Subhash, G., Spearot, D., 2019. Thermodynamics-based stability criteria for constitutive equations of isotropic hyperelastic solids. J. Mech. Phys. Solids 124, 115–142.
Warfield, R.W., Cuevas, J.E., Barnet, F.R., 1970. Single specimen determination of Young's and bulk moduli of polymers. Rheol. Acta 9, 439–446.
Wood, L.A., Martin, G.M., 1964. Compressibility of natural rubber at pressures below 500 kg/cm^2. J. Res. Natl. Bur. Stand. A 68 (3), 259.
Yang, J., Webb, A.R., Ameer, G.A., 2004. Novel citric acid-based biodegradable elastomers for tissue engineering. Adv. Mater. 16 (6), 511–516.
Ye, H., Zhang, K., Kai, D., Li, Z., Loh, X.J., 2018. Polyester elastomers for soft tissue engineering. Chem. Soc. Rev. 47 (12), 4545–4580.
Yeoh, O.H., 1990. Characterization of elastic properties of carbon-black-filled rubber vulcanizates. Rubber Chem. Technol. 63 (5), 792–805.

Yeoh, O.H., Fleming, P.D., 1997. A new attempt to reconcile the statistical and phenomenological theories of rubber elasticity. J. Polym. Sci. B 35 (12), 1919–1931.
Zhang, Y., Yu, K., Lee, K.H., Li, K., Du, H., Wang, Q., 2022. Mechanics of stretchy elastomer lattices. J. Mech. Phys. Solids 159, 104782.
Zheng, Q., Mashiwa, N., Furushima, T., 2020. Evaluation of large plastic deformation for metals by a non-contacting technique using digital image correlation with laser speckles. Mater. Des. 191, 108626.
Zhou, Y., Chen, Y., Jin, L., 2023. Three-dimensional postbuckling analysis of thick hyperelastic tubes. J. Mech. Phys. Solids 105202.